State University of New York The College at Brockport

Palladium Catalyzed Hydrodechlorination of 4-Chloroanisole in Phosphonium Ionic Liquids

Department of Chemistry and Biochemistry

Joseph Hennig
6-24-2016

Table of Contents

Abstract

Until their production was banned in 1979, polychlorinated biphenyls (PCB's), formed as complex mixtures, were used in electrical equipment. Although they are no longer manufactured, some PCBs are still in service—albeit, in closed or semi-closed systems such as dielectric fluids for transformers and capacitors, or are still present in the environment. The continued presence of PCBs is problematic, due to their toxicity. Their hydrophobic nature and resistance towards metabolism leads to bio-accumulation up the food chain. resulting in long term effects in chronically exposed persons, like firefighters, factory workers or persons whose food have accumulated appreciable levels of PCBs. Efficient dechlorination of polychlorinated biphenyls (PCBs) has relevance in the environment, as it would reduce the toxicity of these pollutants. The chemistry described in this thesis is a model study for dechlorinating PCBs using 4-chloroanisole as a model compound. In this fundamental study, palladium-catalyzed dechlorination of chloroanisole was studied in ionic liquids (ILs), where the catalyst was expected to be more stable than in methanol, the previously used solvent. This thesis describes the hydrodechlorination efficacy and longevity of palladium catalysts with ligands **4** (2-(di-tert-butylphosphino)biphenyl) and **5** (2-(di-tert-butylphosphino)-2',4',6'-triisopropylbiphenyl) in methanol and ILs **6** (1-ethyl-3-methylimidazolium bis(trifluoromethylsulfonyl)imide), **7a** (trihexyl(tetradecyl)phosphonium chloride), and **7b** (trihexyl(tetradecyl)phosphonium bis(trifluoromethylsulfonyl)imide) (Scheme 9). Additionally, this thesis focuses on improving the logistical aspects of determining the water content in the ILs, sampling reactions to follow their progress, data reproducibility, and analysis of reaction progress, as well as the impact of water on the rate of hydrodechlorination reactions in ionic liquids. After excluding results from obviously compromised reactions, it appears that reactions in IL **7b** proceed faster on average than those in IL **7a**, that reactions performed with ligand **5** run faster than those with ligand **4**, and that there may be a bell curve to the concentration of water *vs* rate of reaction, with the reaction proceeding best at intermediate water concentrations. Further experiments would be needed to confirm these results.

Introduction

History on PCBs and Detoxification

Compounds that are hazardous to human life are often natural byproducts of living organisms. In fact, polychlorinated biphenyls (PCBs—Figure 1), are surmised to have existed since well-before the industrial era.[1] However, between the 1920's and 1979, manufactured PCBs, formed as complex mixtures, were used in electrical equipment, plasticizers in paints, pigments, dyes and carbonless

Figure 1: Chemical Structure of PCB's. The possible positions of chlorine atoms on the benzene rings are denoted by numbers assigned to the carbon atoms.

copy paper.[2] Since 1979 PCB production has been banned because of its classification as a Persistent Organic Pollutant (POP).[3, 4] Many PCBs that were produced prior to 1979 were dumped into various environments like the Hudson River. Others have not been decommissioned and are in closed or semi-closed systems such as electrical equipment, including dielectric fluids for transformers and capacitors. Some systems containing PCBs have continued in service, in part because of the relatively low acute toxicity, but also the cost of decommissioning.

PCBs are part of a class of compounds considered POPs such as, polychlorinated dibenzo-p-dioxins (PCDDs), and dibenzofurans (PCDFs), whose hydrophobic nature and resistance towards metabolism has led to them bio-accumulating in the food chain. As POPs enter an ecosystem they are ingested by some organism—most often at the bottom of the food chain, such as algae; however, the POPs are minimally metabolized, then persist in that organism until that organism is consumed by a higher organism in the food chain, such as fish. Eventually, these compounds will increase in concentration in the food chain.[4, 5] In fact, many POPs have also been shown to have long term effects in chronically exposed patients, like firefighters, factory workers or persons whose food have accumulated appreciable levels of PCBs.[6, 7, 8] These effects include mild liver failure, or chloroacne. Additionally, acute exposure patients have been shown to develop chloroacne, impairment of liver function,

hematopoiesis, or bronchitis. However, it is unclear whether those acute effects were attributable specifically to PCBs since the oils were also contaminated with dibenzofurans. [8–10] There are more than 400 places in the United States that have PCB contaminated sludge, soil, or creeks, etcetera.[11] Over the last few decades, GE has discharged close to 650 tons of PCBs into the Hudson River. However, in 2015 GE had one of the most successful removals of PCBs from the river processing 2.7 million cubic yards of sediment, removing 100% of the PCBs targeted by the U.S. Environmental Protection Agency.[12,13] This effort consisted of several phases of cleaning, beginning with the removal of the sludge then detoxifying it, and then monitoring the affected sites. This is one of few sites to have been physically cleared, which exposes the necessity for research that would enable the detoxification of these nearly 400 environmentally diverse areas that are PCB-laden.[11]

Many approaches have been suggested for the detoxification of polychlorinated biphenyls and dioxins. There have been many methods explored such as ultrasonically-assisted electroreduction with and without soluble catalysts performing dechlorination of PCBs, anaerobic bacterial mixed cultures performing dechlorination of PCBs and dioxins, other aerobic mixed cultures degrading and mineralizing 3-chlorobiphenyl, or as explored in this paper palladium-catalyzed hydrodechlorination of aryl chlorides as model compounds for PCBs.[14–19] The bacterial dechlorination method explored has been tested in specific ecological systems, mainly in sewer-sludge treatment facilities, and the typical kinetics of these dechlorination methods is on the order of magnitude of days.[15] The success of these methods is notable; however, the development of new chemistry to remove the chlorine substituents from these compounds, decreasing the toxicity of PCBs, is still an important goal. Research that develops additional methods of dechlorination has its own intrinsic benefits; some avenues offer kinetic advancements, some versatility, and some contribute to the understanding of the nature of the catalytic species employed. Likewise, methods for palladium-catalyzed hydrodechlorination like those shown in Scheme 1, have been demonstrated as efficient methods of hydrodechlorination, in controlled environments (air-free, with no contaminants) and still very little is known about the nature of the mechanism.

*Scheme 1: Palladium-Catalyzed Hydrodechlorination of 4-chloroanisole (**2**), in Refluxing Methanol with Ligand **6** or **7***
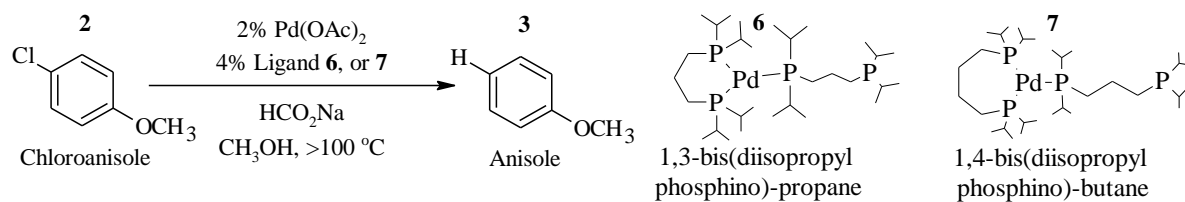
*Adapted from, Milstein, D.; Ben-David, Y.; Gozin, M.; Portnoy, M. J. Mol. Catal. **1992**, 73 (2), 173–180.*

Catalyst History

The current goals for advancing the chemistry presented in this paper involve developing an environmentally friendly hydrodechlorination method that is efficient and cost effective, with relatively stable catalysts, as well as investigating the nature of the reaction mechanism. These goals were explored in Dr. Logan's lab as one of her students, Mark Oinen, began the research by surveying the literature for palladium catalysts for the hydrodechlorination of aryl chlorides. At that time, these catalysts were believed to perform hydrodechlorination on aryl chlorides via a homogeneous (also known as soluble molecular) catalyst. In this model, the transition metal—in this case, palladium—is stabilized by the electron donating centers of a ligand, to the extent that the palladium is still reactive enough to insert into the aryl chloride bond, perform hydrodechlorination, and then regenerate the active catalyst—a homogeneous palladium(0) ligand complex ($Pd-L_n$). Due to the greater strength of the aryl carbon-chloride bond relative to other carbon-halogen bonds, specific ligands were required to generate a palladium catalyst that could insert in them. In one of the first successful methods, published by Milstein, et al., in 1992, they used a palladium catalyst with bulky bidentate phosphorus ligands with sodium formate as the reducing agent in methanol.[20,21] They elucidated that there was a rate-determining oxidative addition of the Pd-catalyst to the aryl chloride, because electron-donating substituents retarded the rates of hydrodechlorination.[20] In 1993, a paper by Portnoy and Milstein described the relationship between the rate of dechlorination and the ratio of the ligand 1,3-bis(diisopropylphosphino)-propane (dippp) and palladium, revealing a slower rate of dechlorination with the addition of excess dippp.[22] Taken together, these two findings revealed that a $14e^-$ Pd(0) intermediate was the most likely state of the palladium catalyst prior to inserting into the aryl chloride bond. For the rate-determining step to be the oxidative addition, and rate retardation to occur with excess ligand, it revealed that an equilibrium exists between a catalyst with a $14e^-$ complex of two monodentate ligands and a $14e^-$ chelated complex. Therefore, increasing the concentration of ligand (dippp), the equilibrium would favor the less reactive monodentate configuration, essentially retarding the reaction (Equation 1).[20,22]

Equation 1: The Equilibrium between a 14e⁻ Chelated Complex and 14e⁻ Monodentate Structure
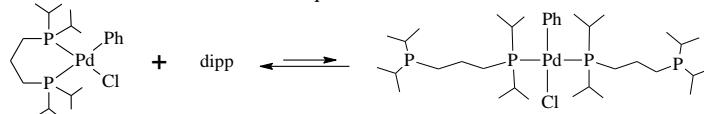
Other research by Portnoy and Milstein supported the claim that the bite angle (P-Pd-P) formed by the chelating ligand and the palladium, had an effect on the rate of reaction.[23] In their research they remarked on the more reactive nature of the Pd(dippp) complex in oxidative addition than an analogous complex with a longer 4-carbon chain separating the chelating phosphorus atoms, Pd[1,3-bis(diisopropylphosphino)-butane], stating that it is likely due to the smaller P-Pd-P angle of the former case.[23,24] They surmised that there were two factors resulting in faster oxidative addition when dippp was used as the ligand. First the bulky ligand favored the 14e⁻ intermediate; and second, the intermediate-sized P-Pd-P angle in the chelate allowed for a stable complex with vacant coordination sites.[23] In total, Milstein, et al., discovered that the necessary ligand for hydrodechlorination using palladium, would be a ligand that complexes with palladium to form an electron deficient active catalyst with sufficient vacant coordination sites.

Despite the Pd(dippp) catalyst's propensity for hydrodechlorination, the ligand was not air stable or commercially available, and the reactions required high temperatures in a sealed reaction vessel. In that same time period, other researchers were also developing palladiumcatalysts that inserted in arylchloride bonds. For example, Hartwig in a 1998 publication presented a procedure for amination of aryl chlorides—using triarylphosphine ligands with palladium, at temperatures between 50-100℃.[25] Then, in a 1999 publication by Buchwald and Wolfe, the use of a highly active catalyst—wherein the ligand was air stable and commercially available, and the catalyst required minimal preparation, reacted at lower temperatures, and appeared to be more efficient— was reported for room-temperature amination and Suzuki-Miyaura coupling of aryl chlorides (Scheme 2).[26]

Scheme 2: General Amination and Suzuki-Mayaura Coupling Schemes
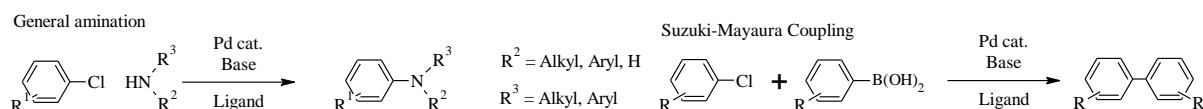
The ligand Buchwald used was a biaryl compound, with a phosphorus having two bulky alkyl substituents on a carbon α to the bond between the two aryl rings. In this ligand, electron donation to the palladium can occur from both the phosphorus lone pair and the π electrons of the other aryl ring. This also allowed for the possibility of substituting the aryl ring to augment the steric effects of the ligand (e.g., in complex **8/12** Scheme 3). At that time, catalyst lifetime studies and systematic assessment of several biaryl ligand substituents had begun with these ligands.[27] Buchwald et al. observed a Pd—C(ipso) interaction (e.g., in complex **12**, Scheme 3) that stabilizes the Pd(0)L$_1$ complex. Buchwald, et al., also noted that this bond might help shift the equilibrium from Pd(0)L$_2$ to Pd(0)L$_1$, a 14-electron complex that undergoes rapid oxidative addition. To evaluate this hypothesis, they prepared the Pd(0) complex, and obtained X-ray crystal structures showing that the Pd(0)L$_2$ complex formed (see complex **11**, Scheme 3) was too sterically hindered to interact with an aryl halide, and also did not allow for the Pd—C(ipso) interaction. However, the propensity for this ligand to undergo oxidative addition had been extensively demonstrated and they proposed that the complex goes through a ligand dissociation forming the active catalyst (Pd(0)L$_1$). Then, they postulated that the Pd(0)L$_1$ complex would form either a 12e⁻ catalyst or 14e⁻ catalyst, depending on the presence of the Pd—C(ipso) interaction. It would form either a 12e⁻ catalyst without the interaction(complex **13,** Scheme 4) and the 14e⁻ (complex **12**, Scheme 4) catalyst with the interaction. Buchwald et al. assert that the 12e⁻ intermediate **13** would be the more reactive toward oxidative addition, and the reaction likely follows through that intermediate like the one suggested in a Hartwig 1995 paper.[27,28] In sum, Buchwald et al. asserted that the electron donating capacity of the phosphorus center is secondary in importance to steric effects from the size of the ligand; essentially, the steric effects can lead to complex **13**, or L$_1$Pd(0)—the more reactive complex.[27]

Scheme 3: Formation of Active Palladium Catalyst from 2-(2',6'-dimethoxybiphenyl)dicyclohexylphosphine and Pd
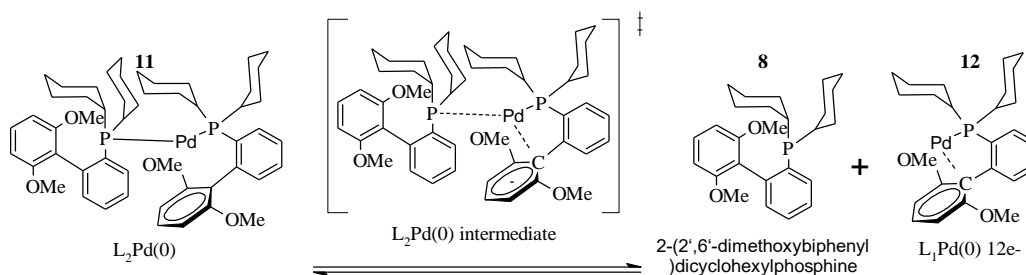
Scheme 4: Oxidative Addition of Aryl Chloride after Dissociation of Phosphine from an L₂Pd(0) Complex in the Suzuki-Miyaura Reaction
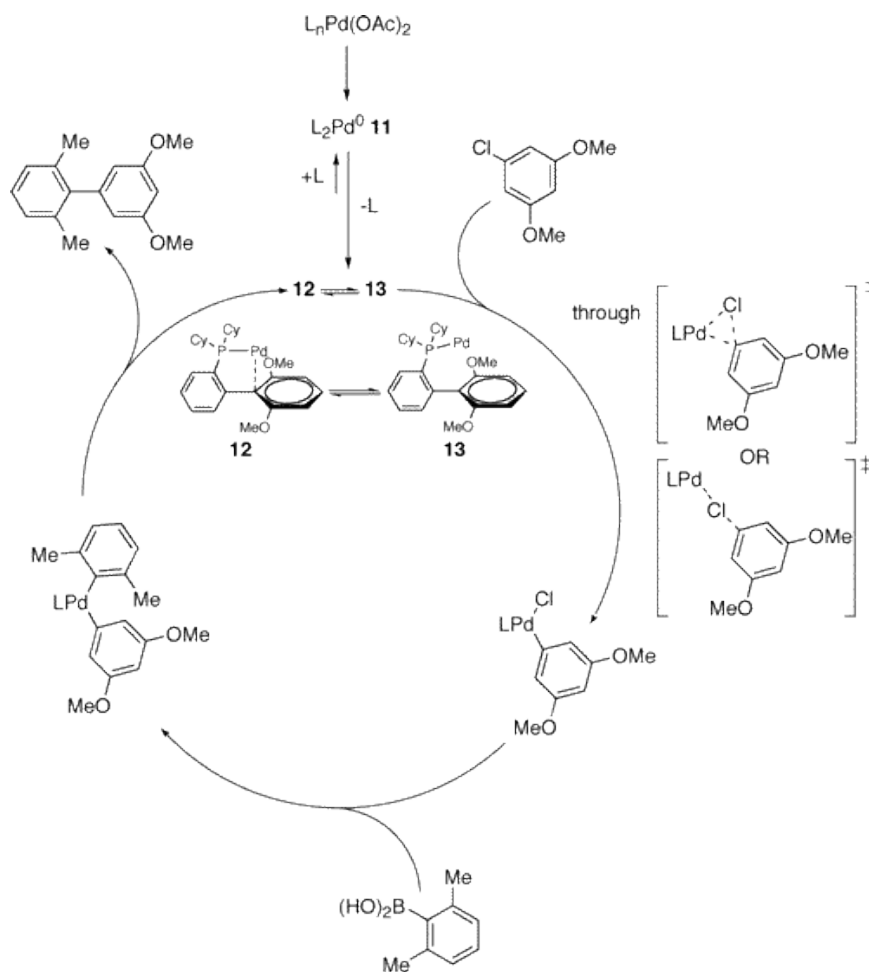
*The inactive ligand Pd(II) complex shown above complex **11** enters the catalytic cycle after Pd(II) is reduced to Pd(0), forming **11**. Then complex **11** dissociates a ligand forming the active complex **12/13**, which undergoes oxidative addition to the aryl chloride. Displacement of the chloride and finally reductive elimination regenerates the active catalyst **12/13**. Buchwald, S. L.; Barder, T. E.; Walker, S. D.; Martinelli, J. R. J. Am. Chem. Soc. **2005**, 127 (13), 4685–4696.*

Incorporating Buchwald Catalysts

The use of Buchwald ligands had been described in amination and Suzuki-Miyaura coupling of arylchlorides, where the chloride was replaced with an amino and an aryl group, respectively (Scheme 2). However, these ligands had not been used in hydrodechlorination. The ongoing studies with Buchwald ligands, as well as their commercial availability and ease of use, made them a particularly attractive candidate for hydrodechlorination. These studies, and the fact that Buchwald ligands had been demonstrated under some conditions to be effective in water in immobilized catalysts,[29] meant that they would also fit with the long-term goals of Dr. Logan's research, performing hydrodechlorination of PCBs in various ecosystems.[18] Therefore, there was ample basis to develop Buchwald ligands for hydrodechlorination.

Mark Oinen and Dr. Logan performed the hydrodechlorination of a series of aryl chlorides as model compounds of PCBs—with a range of electron-donating and withdrawing substituents. They used Buchwald ligand **4** (2-(di-tert-butylphosphino)biphenyl), Pd(OAc)$_2$ as the palladium source, sodium formate as the hydride source, and methanol as the solvent (Scheme 5).[18,20]

*Scheme 5: Palladium-Catalyzed Hydrodechlorination in Refluxing Methanol, Using Ligand-**4** and Sodium Formate*
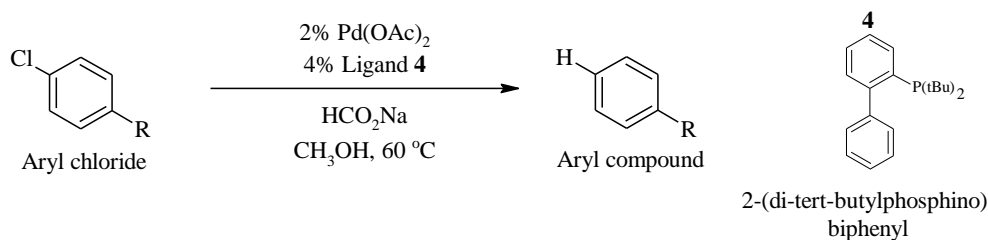
The research revealed that Buchwald ligand **4**, which was air stable and commercially available, performed hydrodechlorination at lower temperatures and in shorter reaction times than was found with (dippp) in Milstein's research.[18,20]
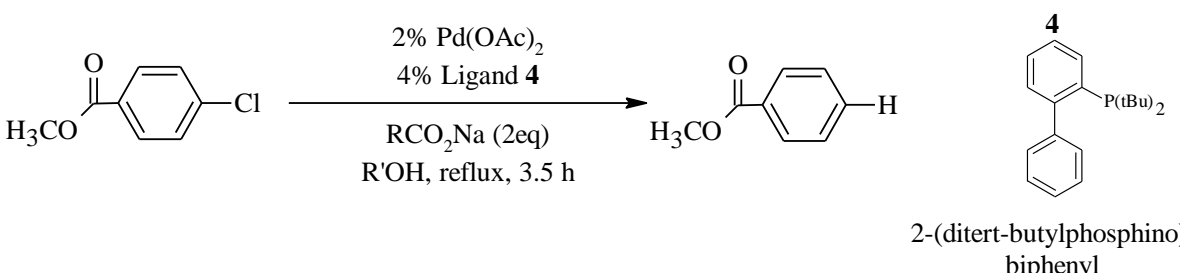
Table 1: Hydrodechlorination of Aryl Chlorides by Scheme 5

Aryl chloride	H$_3$CO—⟨⟩—Cl	H$_3$CO(C=O)—⟨⟩—Cl	(C=O)—⟨⟩—Cl	(O=C)—NH—⟨⟩—Cl	naphthalene-Cl
Time, h[a]	3	1.5	2	3	4
Yield, %[b]	99	97	100	97 (89)	95 (90)

[a] *Average of two runs.* [b] *GC yields, average of two runs (isolated yields). Adapted from; Logan, M. E.; Oinen, M. E. Organometallics **2006**, 25 (4), 1052–1054.*

This research also improved Milstein's reaction scheme by showing more consistent reaction times when the reaction was allowed to form what was believed to be the active catalytic complex, by stirring the $Pd(OAc)_2$ and ligand in a portion of methanol solvent for 5 minutes prior to the addition of the substrate, reducing agent, and remaining solvent. Additionally, sodium formate was confirmed as the hydride source for this reaction—as opposed to methanol—by making a three-way comparison. Results from the standard reaction conditions, a reaction with the base changed to sodium acetate, and a reaction with the solvent changed to tert-butyl alcohol, showed that changing the solvent did not have an impact on the reaction leading to 90% conversion in 1.5 h, but changing the base led to 5% conversion in 1.5 h (Table 2).

Table 2: The Hydride Source in Hydrodechlorination

2-(ditert-butylphosphino) biphenyl

R	R'	% conversion [a]
CH$_3$	CH$_3$	5
H	(CH$_3$)$_3$C	90
H	CH$_3$	97 [b]

[a] GC yield. [b] 1.5 h reaction time, from Table 1. Adapted from; Logan, M. E.; Oinen, M. E. Organometallics **2006**, 25 (4), 1052–1054.

Deciphering the Nature of the Catalyst

Traditionally, heterogeneous and homogeneous catalyst mechanisms were considered distinct; meaning that reactions could be classified as proceeding through one mechanism or the other. Heterogeneous catalysts would be described as being in a separate phase from the substrate, and homogeneous catalysts would be described as being in the same phase. An example of heterogeneous catalyst is Pd/C for hydrogenation of alkenes, while the catalyst in the Heck, or Suzuki-Miyaura reaction was believed to be homogeneous. However, there were questions beginning to arise in the literature concerning the strict dichotomy that was thought to exist between heterogeneous and homogeneous palladium catalysts. In fact, at this time, de Vries,[30] Reetz,[31] DuPont,[32] Finke,[33] among others, suggested that most Heck and Suzuki reactions were actually proceeding through catalysis in which the form of palladium was between heterogeneous and homogeneous. In a 2006 review Jones, et al., state that regardless of the reaction conditions, most Heck and Suzuki reactions were being understood as having a reservoir of nanoparticulate palladium—palladium colloids between 1-7 nm in diameter—that feed the homogeneous active catalysis (Scheme 6).[32,34] At this time, Dr. Logan and her student Cory Charbonneau began doing research on the nature of the active catalyst in the hydrodechlorinations, as it might exist as homogeneous, both nanoparticle and homogeneous, nanoparticle, or heterogeneous palladium catalyst [30–37] even though the catalysts were originally thought of as purely homogeneous or heterogeneous.

Scheme 6: Possible Pathways Involved in the Heck Reaction Promoted by Palladium Nanoparticles
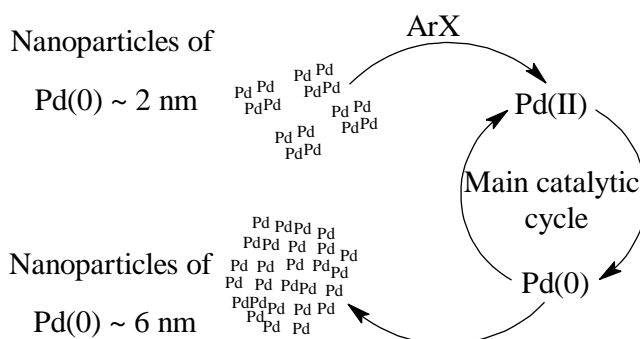
*Adapted from: Dupont, J.; Cassol, C. C.; Umpierre, A. P.; Machado, G.; Wolke, S. I. J. Am. Chem. Soc. **2005**, 127 (10), 3298–3299*

Another incentive for examining the nature of the active catalyst was that it had been suggested that nanoparticulate palladium is stabilized by ionic liquids (ILs).[32,38] Essentially, if the

hydrodechlorination method used by Dr. Logan's lab was mechanistically proceeding through a unification of nanoparticulate colloids and homogeneous active catalysis with Pd(0), then ILs could potentially stabilize the reservoirs of Pd nanoparticles, reducing their tendency to aggregate further into elemental Pd (Pd black), and perpetuate the reaction. It was hypothesized that if the reaction proposed by Dr. Logan's lab (Scheme 7) was impacted by the structure of the ligand, that would provide evidence for the existence of homogeneous catalysts in the reaction, but not evidence for nanoparticulate palladium. Although that experiment would not provide evidence for nanoparticulate palladium, it also would not rule out the presence of nanoparticulate palladium in the reaction. In an effort to assess the nature of the active catalyst, Charbonneau compared the impact of various ligands on the reaction rates, and then performed mercury-poisoning experiments like those described in Finke and Widegren, and Phan et al.,[33,34] to determine if there were, indeed, nanoparticulate palladium colloids in the reaction. (Additional studies that were considered but have yet to be pursued in Dr. Logan's lab, included but were not limited to TEM, kinetic studies, phosphorus NMR and homogeneous catalyst poisoning, such as the Crabtree's test.[33,34])

Scheme 7: Proposed Mechanism of a Pd(0) Intermediate Facilitated by Ligands in Palladium-Catalyzed Hydrodechlorination
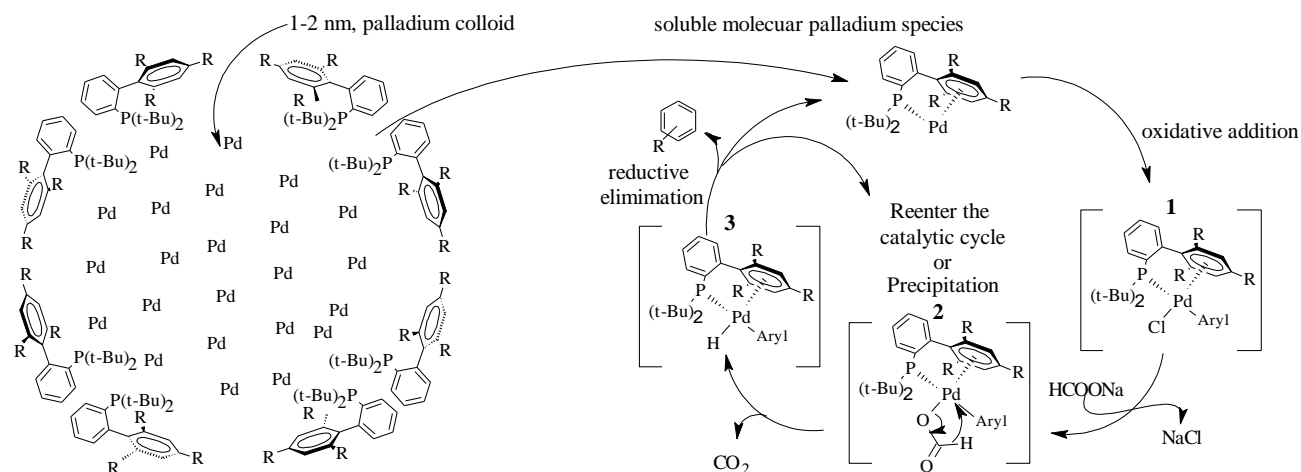
*A reservoir of palladium supplies the ligand to form the homogeneous Pd(0) species, which oxidatively adds to the aryl chloride—followed by ligand substitution with the formate anion and the release of NaCl—forming intermediate **2**. Decarboxylation of intermediate **2** delivers intermediate **3**. The final product is formed via reductive elimination with the regeneration of Pd(0) homogeneous species, or precipitation of palladium black. Adapted from Zhang, C.; Li, X.; Sun, H. Inorganica Chim. Acta **2011**, 365 (1), 133–136*

Charbonneau ran hydrodechlorination reactions in methanol with three ligand structures, **4**, **8**, and **9** (Table 3), and showed that the ligand structure has an impact on the rate (Table 3). These ligands capitalized on the ability to vary the steric and electronic effects of the ligand by substituting the phosphorus with cyclohexyl groups (Ligand **9**, Table 3) or substituting both the phosphorus with cyclohexyl groups and the aryl ring with methyl groups (Ligand **8**, Table 3). Ligand **4** ran to completion in 3 hours at approximately 39.9% per hour, ligand **8** ran at approximately 10.8% per hour—which likely ran to completion before sampling at 24 hours—and ligand **9** ran at 2.8% per hour and only reached 79% at 52 hours. While these were tentative results—needing more replication— they still provide evidence for the impact of ligand structure on the rate of reaction, and confirmed Mark Oinen's previous results that ligand **4** performed better than **9**.[18] A simple reaction that would give strong evidence for nanoparticulate palladium as the active catalyst would be comparing the rates of a reaction with and without a ligand. Charbonneau ran these experiments without ligand: it was shown that they ran relatively fast in methanol, but halted at 11%. This revealed that there was some baseline activity from the palladium, but it was not sustained without the ligand. However, now Charbonneau had provided evidence for homogeneous catalysis in the ligand experiments; therefore, they decided to perform mercury-poisoning experiments, in hydrodechlorination and amination reactions, to provide more quantitative evidence for or against the nanoparticulate component. Mercury poisoning was performed in; hydrodechlorination reactions using IL **7b** or methanol as the solvent; and amination reactions using IL **7b** or toluene as the solvent (as in Scheme 2). Mercury(0) forms an amalgam with nanoparticulate palladium(0). Therefore, any reaction that is stopped or slowed by the addition of mercury(0) will have been using palladium(0) in its nanoparticulate (or Pd black) form at some point in the catalytic cycle.

Table 3: Rates of Dechlorination in Methanol with Varying Ligand Structures

Time (h)	% yield	Time (h)	% yield	Time (h)	% yield
0.5	5	1	26	1	6
1	5	2	34	4	14
2	49	4	63	22	51
3	100	6	78	48	77
24	100	24	98	52	79

*Adapted from Cory Charbonneau's unpublished **2006** results.*

Charbonneau's work in Dr. Logan's lab demonstrated that hydrodechlorination using ligand **4** in

IL**7b** (Figure 2, panel **A**) and methanol (Figure 2, panel **B**), with mercury(0) added, caused immediate

reaction cessation, compared to the control without mercury added, which is a positive indicator of

nanoparticulate palladium(0). Then he ran the amination reactions, that were previously considered

homogeneous, with 4-chloroanisole and morpholine as the reactants in both IL **7b** (Figure 2, panel **C**) and

toluene (Figure 2, panel **D**). When mercury was added, those reactions ceased, compared to the control

amination reactions without mercury. This indicated that the amination reaction, previously accepted as

purely homogeneous, also used nanoparticulate palladium(0) in its catalytic cycle.

Figure 2: Mercury Poisoning Experiments in Various Solvents
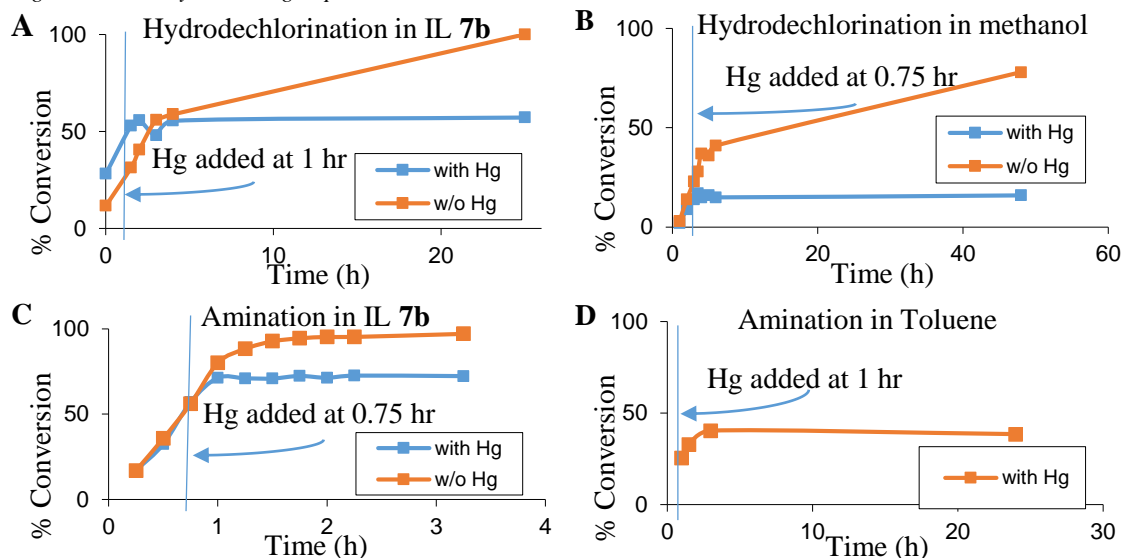
*Adapted from Corey Charbonneau's unpublished **2006** results.*

If the active catalyst in the reaction were homogenous then the reaction rate would rely on the ligand, and the reaction would not cease with the addition of mercury. Conversely, if the active catalyst were nanoparticulate, then the rate would not depend on the ligand, and the reaction would cease with the addition of mercury. In fact, mercury poisoning was initially developed to distinguish between heterogeneous and homogeneous reactions, [39,40] and at the time that Charbonneau was performing these experiments, its credibility was being questioned.[34] Mercury poisoning certainly will only react with unbound palladium(0) forming an amalgam, [39,40] but the results were now confounded by the concept of nanoparticulates feeding the reaction [32,34]—which is supported by differing reaction rates when utilizing different ligands. From the results of Charbonneau's and Dr. Logan's research they postulated that both the homogenous component and the nanoparticulate might be in equilibrium with each other. The ligand might be allowing the palladium to exist in small nanoparticulate colloids, avoiding palladium precipitation (to palladium black), which other labs have visualized in electron microscopy.[32,41] This helps to explain that the rate of reaction is affected by the ligand because the active catalyst is ultimately a homogeneous species taking palladium(0) from nanoparticulate colloids to oxidatively add to the aryl chloride.

However, another explanation might be that the palladium-ligand complex is not as stable as the amalgamation product [34,39,40] and mercury actually can "steal" the palladium from the ligand, but this seems to be excluded by work with TEM microscopy.[32,41] In total, the positive mercury poisoning results do not exclude the idea that the catalyst is homogenous in nature, despite the impact of the ligand on the rates of reaction; and the poisoning of the reaction by the addition of mercury. Therefore, as Charbonneau's and Dr. Logan postulated, and is currently the accepted hypothesis; the ligands coordinate to palladium(0) from a colloid—forming the active catalyst—which oxidatively adds to the substrate, entering through the catalytic cycle (Scheme 7).[42]

Experimental Difficulties

Throughout the work that Dr. Logan's lab had done up to this point there were several factors that would complicate the collection of experimental data and data reproducibility. The most problematic factors that were identified at that time were the slow reaction initiation times, and evaporation of methanol over the course of the reaction. Charbonneau and Dr. Logan had worked on stirring the palladium and ligand for 5 minutes prior to beginning the reaction, to 'initiate' the catalyst, allowing it to form the active species. This made the reaction start time slightly faster, but it was still inconsistent. Fortunately, at this time there were new ligands that had been developed by the Buchwald group to solve this specific problem.[43] Both the new ligands and a set of inactive precatalysts containing palladium and these new ligands (Figure 3) were reported to have longer catalyst life. These precatalysts, with base treatment, would yield the active catalyst eliminating the question of reaction initiation.

Figure 3: Novel Precatalysts, and Ligand[43]

2-ditert-butylphosphino-2',
4',6'-triisopropylbiphenyl
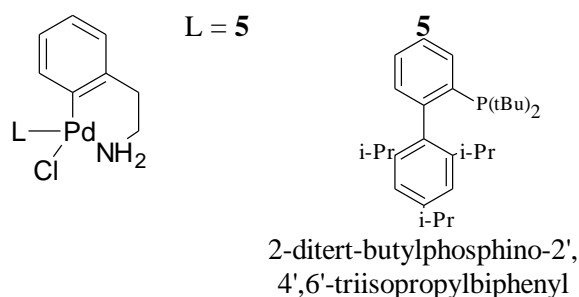
The development of ligands having improved catalytic ability and the ability to generate the active catalyst from a pre-catalyst provided the potential for improvement over the results previously published by Dr. Logan, because of the potential of improved reaction initiation.[44] These precatalysts were explored by Dr. Logan's student, Dan Zdanowski for hydrodechlorination in methanol. His results showed that the pre-catalysts were ineffective in the hydrodechlorination chemistry, resulting in immediate precipitation of palladium black. Alternatively, while using methanol as the solvent, the newer ligand—not as a precatalyst—resulted in faster but less stable catalytic systems; essentially, the catalyst from ligand **5** gives a faster rate but deactivates more quickly (Figure 4).

Figure 4: Catalyst Life Studies at 63˚C in Methanol
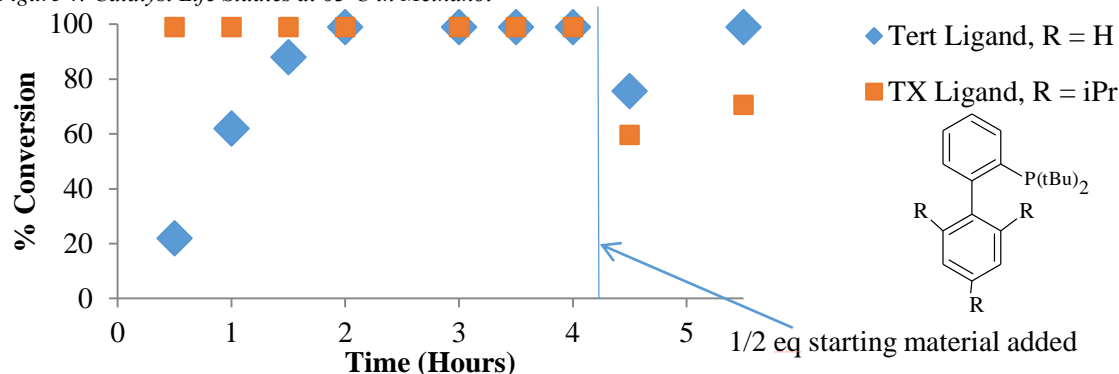
Unpublished results from Dan Zdanowski in Dr. Logan's lab.

The literature provides support for the use of ILs as solvents in palladium-catalyzed reactions ,[45] and

recent work has shown that in ILs, the palladium is in a nanoparticulate form, existing in small clusters

(Scheme 6).[32,41,46] The ions of the IL are believed to stabilize these clusters, and keep them from

precipitating as palladium black. Additionally, these ILs are considered to be more environmentally

friendly solvents than methanol or toluene, because they are less volatile—which also helps by reducing

the evaporation of the solvents, making them more likely to preserve the catalyst.

This thesis will describe the use of ILs **6**, **7a** and **7b** (Scheme 8)—while using catalyst systems

containing Buchwald ligands, including ligands **4** and **5**—in hydrodechlorination reactions. Additionally,

this thesis will discuss the development of NMR data analysis, other possible avenues of data analysis,

the water content of the reactions, sample evaporation, sampling techniques, investigation of the nature of

the active catalyst, and improvements on the logistical aspects of data reproducibility.

Scheme 8: Hydrodechlorination in Methanol or Ionic Liquid (IL)
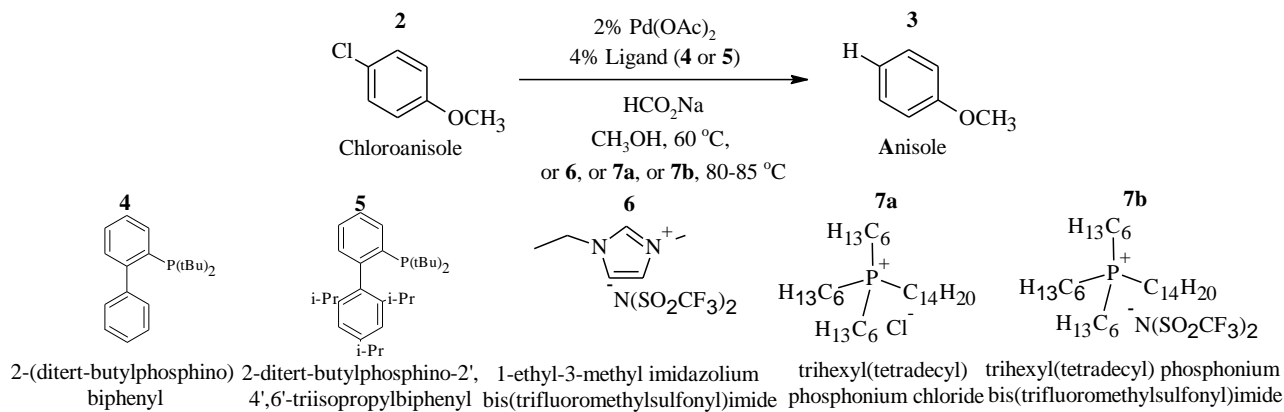
Experimental Section

General

Unless otherwise stated, commercially obtained materials were used without further purification. TMS, acetone-d_6, DMSO-d_6, and CDCl$_3$, were used as received. In the case of acetone-d_6, and DMSO-d_6 4Å molecular sieves were added once opened. For samples in which TMS was used as a reference, it was added to the CDCl$_3$. The methanol solvent was either Sure/Seal, purchased from Sigma Aldrich, or AcroSeal, purchased from Fisher Scientific. Ionic liquid (IL) **7a**, was donated by Cytec and used as received unless otherwise stated. IL **7b** was prepared by the reaction of IL **7a** with commercial lithium bis(trifluoromethanesulfonyl) imide from Acros in an aqueous-organic workup.[47] Anhydrous sodium formate 99.98% was purchased from JT Baker Chemical Co. Pd(OAc)$_2$ was purchased from Strem, 99+%. Ligand **4**, and **5**, 99%, were purchased from Strem. Silica gel, 230-400 Mesh, was purchased from Fisher Scientific. All materials were weighed on an AG104 Mettler Toledo analytical balance.

Nuclear magnetic resonance spectra were recorded on a Bruker Avance 300 MHz instrument. All ^{1}H NMR data are reported in δ units, parts per million (ppm) relative to the residual protons in a deuterated solvent (CDCl$_3$ 7.26 ppm, (CD$_3$)$_2$CO 2.05 ppm, or DMSO 2.5 ppm). Gas chromatographic analyses were performed on a Hewlett Packard 6890 series, gas chromatography instrument with an FID detector using a 30.0 m length x 320.0 µm diameter capillary column with 5% Phenyl Methyl Siloxane as a 0.25 µm thick stationary phase. A Mettler Toledo C20 Coulometric Karl Fischer titrator was used in all water analysis unless otherwise noted.

All reactions were carried out under an argon atmosphere, unless otherwise noted. The vacuum used was house vacuum, ~30 mmHg, unless otherwise noted. All reactions in methanol were analyzed using GC analysis. All reactions in IL, unless otherwise stated, were analyzed with ^{1}H NMR, and sometimes with ^{13}C NMR. Prior to setting up reactions or sampling, all reusable glassware was heated at 100 ℃ in a vented oven. Hamilton gas tight syringes used were, 100 µL, 250 µL, 500 µL, and 1000 µL. Drummond Scientific Company Wiretrol disposable pipets were used for sampling the reactions and were not reused.

Experimental 1. Drying the Ionic Liquid (IL) Under Vacuum

A two-neck 100 mL flask was equipped with a glass stopper on the side neck, and a stopcock with a 0.25 inch wall thickness rubber hose attached to the vacuum pump on the main neck (Figure 11). A stir bar was added to the flask with the IL to be dried, then the IL was heated to 85 °C under vacuum in a silicone oil bath for 24 hours while stirring. The flask was allowed to cool under vacuum, the stopcock was closed, plastic Keck clamps were added to each joint, and the flask was removed from the vacuum line then filled with argon. A septum was attached to a 1 mL gas-tight water-free syringe (Figure 11) which was used to remove 1 mL of liquid for the neat Karl-Fischer titration (Experimental 3)

Experimental 2. Determination of Water by Karl-Fischer (10:90 IL: Methanol)

Using a 1000 µL gas-tight syringe and an argon blanket, 1 ml of methanol was removed from an AcroSeal anhydrous methanol bottle. The syringe was quickly tared. After taring, 100 µL injections were analyzed in Karl-Fischer titration, taring between each consecutive injection. A 10% (by mass) solution of IL and methanol was mixed into a 0.5 mL evacuated and argon flushed vial. a gas-tight syringe was weighed, 100µL of solution was drawn into the syringe, it was weighed, and then injected into the Karl-Fischer titrator. After injection, the syringe was weighed again. Nine sequential trials were run. From the titration data, mass percent, χ_{H_2O} (mole fraction), and the standard deviation were calculated and recorded. The IL may be pumped again (Experimental 1) if the water content is not within the desired range.

Experimental 3. Determination of Water by Karl-Fischer (Neat); Preferred Method

A 1000 µL gas-tight syringe, with a 14-gauge needle was used to withdraw 1 mL of the dried IL under argon. The syringe tip was changed to a 22-gauge needle, 100 µL discarded then the syringe was tared. After taring, 100 µL injections were analyzed in Karl-Fischer titration, taring between each consecutive injection. From the titration data, mass percent, χ_{H_2O} (mole fraction), and standard deviation were calculated and recorded with every trial. The IL may be dried again if the water content is not within the desired range.

Experimental 4. Optimized General Procedure, Hydrodehalogenation of 4-chloroanisole in IL

The IL was heated under vacuum and analyzed for water, then kept under argon. A 25 mL two-neck flask containing a magnetic stir bar was evacuated and refilled with argon five times, using house vacuum and argon connected to a dual manifold. To this flask, IL (2 mL) was added using a 1000 µL gas-tight syringe attached to a rubber septum (Figure 11). The flask was then evacuated and refilled with argon three additional times. First, the ligand **4** (4.8 mg, 0.016 mmol) or **5** (6.8 mg, 0.016 mmol), and Pd(OAc)$_2$, (8.98 mg, 0.04 mmol) (Pd-L) were weighed in a polystyrene boat, then using weigh paper, as a static free funnel, the Pd-L were added directly into the IL with excess argon flow. The mixture was stirred until the Pd-L fell to the bottom of the flask, and then the flask was evacuated and refilled with argon 3x while heating them in IL at ≈65 ℃, for 1 hr unless stated otherwise. Second, anhydrous sodium formate (272 mg, 4 mmol) was weighed and added using the previously described techniques, and then 4-chloroanisole (285 mg, 245 µL, 2 mmol) was added using an argon-flushed 250 µL gas-tight syringe. Flushing with 4-chloroanisole also allows for the sodium formate to be pushed into the bottom of the flask. After the addition of chloroanisole, the flask was evacuated and refilled 2x more with argon, the temperature of the silicone bath was increased to 80 ℃, and the reaction was allowed to proceed. Samples were taken as described in Experimental 5.

Experimental 5. NMR Analysis

Once the reaction had begun, reaction samples were collected at appropriate time intervals. This was done quickly, using 50 µL Wiretrol disposable pipets—attached to a septum like the septum in Figure 11—while the flask was being lightly flushed with argon. These samples were dissolved in 600 µL of CDCl$_3$ and analyzed by 300 MHz ^{1}H NMR The ^{1}H NMR analysis relied on integration and multiplicity. The NMR spectra were interpreted as described in Results and Discussion section 2.

Experimental 6. GC Sample Preparation, with Filtration Column; with Methanol Solvent

Figure 5: Micro Column
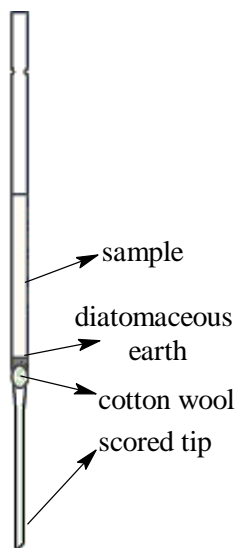
Reactions were set up as described in Experimental 4. The reactions were run with equivalent reagent quantities, but the reactions were run in methanol (2 mL) and not IL. Then, to analyze a sample of a reaction without harming the GC instrument, a Pasteur pipet was scored, and broken to widen the tip enough to make a micro column. The 'column' was comprised of the widened pipette, with a piece of cotton wool in the tip, and a layer of diatomaceous earth above it (Figure 5). To determine if the sample had cleared through the 'column' a TLC plate was spotted at intervals with samples of the eluate, and scanned for UV activity. After the sample was cleared through the 'column' and added to a GC vial, the sample was analyzed. The GC results were analyzed by creating standard samples, running one vial with anisole and a different vial with 4-chloroanisole, then another with both to compare the resulting peaks and determine the retention times of products, reactants, and solvent.

sample

diatomaceous earth

cotton wool

scored tip

Experimental 7. Column chromatography, TLC, NMR, Baeyer's Reagent Test for IL, Phosphine, or Alkenes, and GC Analysis

Another experimental procedure that was explored was the use of GC analysis for hydrodechlorination reactions in IL. A miniature column was prepared using a glass pipette with a scored tip, which had cotton in the end, then silica gel (230-400mesh, 40-63 μm) was placed in the column, and a small round piece of filter paper was placed on top. The column was loaded using 99:1 C_6H_{12}:CH_2Cl_2 with a 0.2 mL of IL **7a** containing 1 drop of 4-chloroanisole/anisole. Then the column was flushed with 98:2 C_6H_{12}:CH_2Cl_2, and the eluate collected in several 1 mL vials. Each vial was tested for UV activity, on a TLC plate. A TLC was run of the UV-active fractions to test for the presence of IL in the UV active eluent, which would indicate IL traveling with chloroanisole or anisole through the column. The TLC would reveal whether there was any sample remaining at the spotting origin, which would most likely be residual IL. If the TLC suggested IL being present, an NMR of the eluate was run. Then if the NMR analysis suggested IL being present a second TLC was done using 98:2 C_6H_{12}:CH_2Cl_2 ; the first lane was spotted with **2**, the second **3**, the third 99:1 **C_6H_{12}:CH_2Cl_2**, the fourth IL **7a**, the fifth **CH_2Cl_2**, the sixth CDCl$_3$ (Figure 6). Then the eluted plate was briefly submerged in Baeyer's reagent (basic KMnO$_4$ solution) and allowed to develop, to determine if the NMR was actually visualizing alkenes from β-elimination on the phosphonium cation. If the NMR, TLC, or Baeyer's reagent was convincing that no IL was present, GC was used to analyze the constituents of the eluate—assessing the purity of the solvent and ratio of anisole to 4-chloroanisole.

Experimental 8. Attempt to Perform and Monitor the Hydrodechlorination Reaction in an NMR Tube
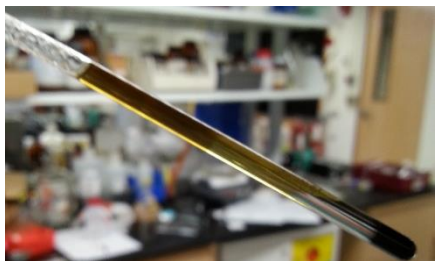
The ligand **4** (4.8 mg, 0.016 mmol) or **5** (6.8 mg, 0.016 mmol), and Pd(OAc)$_2$, (8.98 mg, 0.04 mmol) (Pd-L), were added to a pestle and ground with a mortar, until seemingly homogeneous, then 1/3 of the mixture (13.8 mg with **4** or 15.8 mg with **5**) was added to a 7-inch NMR tube with a valve. Then sodium formate (90.7 mg, 1.33 mmol) was added using a polystyrene weigh boat and weigh paper as a funnel, then the tube was capped and evacuated and refilled with argon 3x. Then, while flushing the tube with argon and using a Wiretrol disposable pipet, IL (1.33 mL) was added to the NMR tube and the tube was evacuated and refilled with argon. Then the tube was shaken, and sat until the IL mixed with the ligand catalyst mixture. Once the IL drained to the bottom, a gas-tight syringe with a 22-gauge needle was used to inject 4-chloroanisole (95 mg, 81.7 µL, 0.667 mmol), after which the NMR tube was submerged in an 80 ℃ oil bath, and monitored by NMR at intervals.

Experimental 9. Preparation of IL 7**b** (trihexyl(tetradecyl) phosphonium bis(trifluoromethylsulfonyl)imide)

Lithium bis (trifluoromethanesulfonyl) imide (10.0 g, 0.035-mol) was weighed into a tared 250 mL Erlenmeyer flask with a stir bar as in Del Sesto et al., 2005.[47] Then H$_2$O (120 mL) was added to the salt. IL 7**a** (18.1 g, 0.035 mol) was added to CHCl$_3$ (180 mL) in a 250 mL Erlenmeyer flask with a stir bar. After 10 mins, of stirring each mixture they were added to a 500 mL Erlenmeyer flask. The original flasks were rinsed with 50 mL of their respective solvent and added to the 500 mL Erlenmeyer flask. A large stir bar was added and the mixture mixed overnight. If an excess of phosphonium IL were added by mass (due to the viscosity of **7a**, it was difficult to obtain a particular mass), extra lithium salt was added. After stirring overnight, the reaction was placed into a 500-mL separatory funnel, and shaken. The layers were separated, and the organic layer was washed with portions approximately 50 mL of H$_2$O until no chloride ion was detected in the wash by a 0.1 M silver nitrate test. The resulting organic layer was drained into a 1000-mL round bottom flask, rotovapped, and then heated at 85℃ on a vacuum pump until

Karl Fischer titration confirmed a dry IL (0-200 ppm). Then NMR analyses (Table 20) were performed to confirm purity and the absence of CHCl$_3$.

Experimental 10. Analysis of Water Content in Sodium Formate
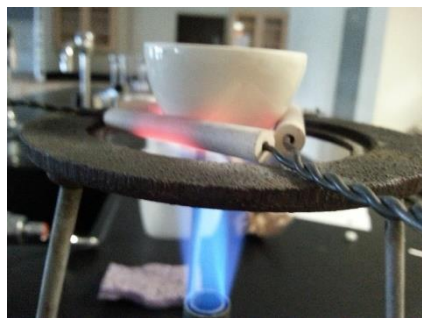
A crucible was preheated using a medium intensity flame, and then a cover was placed on the crucible while it cooled. The crucible was massed, and sodium formate (0.272 g) was added. Once the sodium formate was added, the mass was recorded every minute for 5 minutes, then it was placed above the burner and heated (slowly increasing the flame until at the height depicted in the picture). The crucible was covered again and allowed to cool, and then the crucible was weighed to determine the mass of water lost. This mass of water was calculated by adjusting for the appropriate stoichiometric equivalencies (see, results and discussion section, 9).

Experimental 11. Double-Sized Hydrodechlorination of 4-chloroanisole in IL**7a** Using Ligand **4**

A reaction was set up as explained in Experimental 4, with the exception of having 8 mol% ligand with 4 mol% Pd(OAc)$_2$, and 8 mmol of anhydrous NaCO$_2$H with 4 mmol of 4-chloroanisole—essentially doubling the size of the reaction. The results were collected via NMR, and described in the conclusion of the results and discussion.

Results and Discussion

This project has several long-term goals, one of which is to develop procedures for palladium-catalyzed hydrodechlorination of aryl chlorides that would eventually be appropriate for soil and water treatment in areas of PCB and dioxin contamination. Another long-term goal is to use environmentally friendly solvents for palladium-catalyzed hydrodechlorination of aryl chlorides, that would also lengthen the catalytic efficacy. This paper focuses on the development of a palladium-catalyzed hydrodechlorination in ILs. The plan was to test the hydrodechlorination efficacy and longevity of palladium active catalyst with ligands **4** (2-(di-tert-butylphosphino)biphenyl) and **5** (2-(di-tert-butylphosphino)-2ʹ,4ʹ,6ʹ-triisopropylbiphenyl) in methanol and ILs, **6** (1-ethyl-3-methylimidazolium bis(trifluoromethylsulfonyl)imide), 7**a** (trihexyl(tetradecyl) phosphonium bis(trifluoromethylsulfonyl)imide), and 7**b** (trihexyl(tetradecyl) phosphonium chloride) Scheme 9.

Scheme 9:Hydrodechlorination in Methanol or Ionic Liquid (IL)
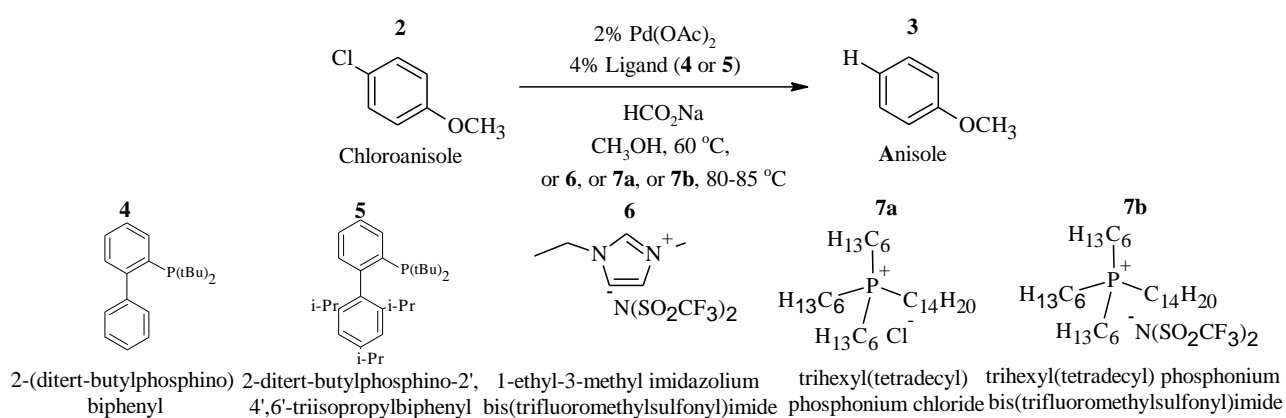
1. Confirming Previous Results in Methanol

The initial experiments were done with Shawn Dirx, another of Dr. Logan's research students, whose reactions are referenced starting with SAD, as mine are with JDH. We confirmed reactions in methanol were comparable to studies done by previous students in Dr. Logan's lab.[18] Although we meant to use the same conditions as used by previous students (Scheme 9), we inadvertently used 20% of the original ligand concentration (0.8-mol %) with $Pd(OAc)_2$ (2-mol %), sodium formate (4 mmol), 4-chloroanisole (2 mmol), and methanol (2 mL), at 60℃ (Scheme 10). Despite the differences between amount of ligand, the reactions that we set up (**R_{xn}'s 1 & 2**, Table 4) had results comparable to previous experiments by Dr. Logan's lab with a ligand amount of 4-mol %—also in methanol. Due to similar reaction times between **R_{xn} 1 & 2** (Table 4), and earlier experiments (Table 3), this lower amount of the ligand was used in subsequent reactions. Of note, we performed duplicate reactions, in part to confirm that the results were consistent, but also for ease of setup. Although my and Sean's results were similar, between **Rxn 2:F** and **Rxn 2:G**, the latter reaction was more complete. This was possibly due to inconsistency in initiation, and we continued working to improve our data reliability.

Scheme 10: Hydrodechlorination in Methanol or Ionic Liquid (IL), with 20% of the Original Ligand Concentration
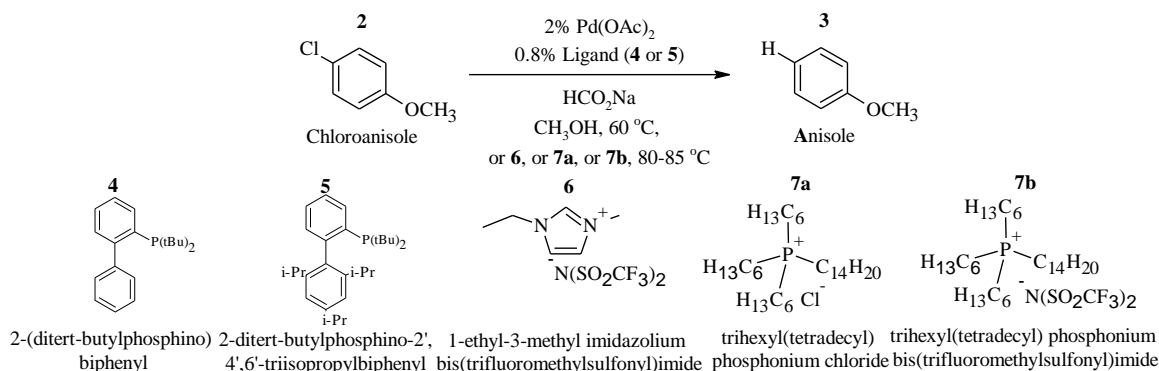
Table 4: Hydrodechlorination in Methanol Comparing Ligands 4 & 5, GC Dissolved in Methanol

R_{xn} name		Reference	Ligand	Intl. comp.	Time	Temp ℃	Rxn solv.	Solvent	Analysis	% Conv.	ppm H_2O
1	A	SAD6A	4	2	02:00	60	CH_3OH	CH_3OH	GC	28	N/A
	B	JDH3C	4	2	02:00	60	CH_3OH	CH_3OH	GC	24	N/A
2	C	SAD7C	5	2	00:30	60	CH_3OH	CH_3OH	GC	31	N/A
	D	JDH5C	5	2	00:30	60	CH_3OH	CH_3OH	GC	22	N/A
	F	SAD8A	5	2	02:00	60	CH_3OH	CH_3OH	GC	67	N/A
	G	JDH5C2	5	2	02:00	60	CH_3OH	CH_3OH	GC	93	N/A

The ppm of H_2O was a later addition to the research, and the water content of all the reactions are discussed in results and discussion sections 4, and 8. JDH5C2 was the second run of JDH5C0022 because the original data were distorted.

With methanol as the solvent, GC was used to analyze the reaction progress. We made standard chromatograms to ensure proper GC analysis (Chromatogram 1, Table 5). The GC standards of 4-

chloroanisole and anisole—assuming that the two compounds were responding identically in the flame ionization—showed retention times of 5.47 minutes, and 3.84 minutes respectively. For the hydrodechlorination reactions, the peaks that resolved at those retention times were integrated, and percent conversion was tabulated by dividing the anisole integration by the sum of the two integrations.

Chromatogram 1: GC Chromatogram of 4-chloroanisole, and Anisole Standards
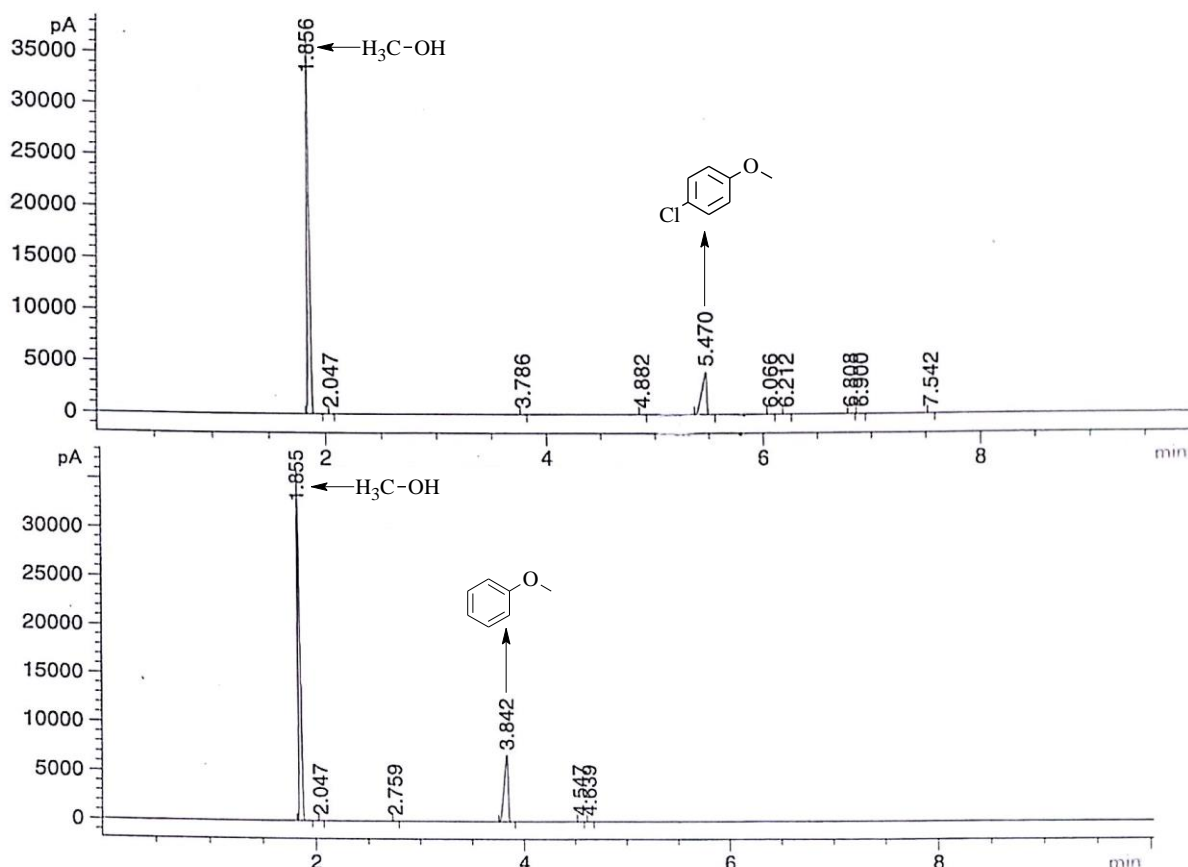
Retention time of 5.470 minutes was assigned to 4-chloroanisole based on the top spectra only containing 4-chloroanisole and methanol, then 3.842 minutes was assigned to anisole based on the same criteria.

Table 5: Conditions and Filenames of 4-chloroanisole, and Anisole Standards

Reference	Intl. comp.	Temp °C	Solvent	Analysis	Misc. info
JDH3A	3	25	CH₃OH	GC	Standard
JDH3B	2	25	CH₃OH	GC	Standard

2. Development of the NMR analysis

Despite the minor inconsistencies, we had similar reaction rates compared to previous student's work in Dr. Logan's lab. At this time, we wanted to transition to ILs as solvents for the hydrodechlorination because of the possibility of longer catalyst lifetime by preserving the activated catalyst, through preventing palladium black formation, and for the environmentally friendly nature of the IL solvents compared to methanol. Perhaps catalyst longevity should have been explored in detail given the different ligand concentration. Nevertheless, prior to beginning the experiments, an efficient analytical method had to be established to follow reaction progress. When the reaction was performed in methanol, the analysis was done with GC; however, when changing to IL as a solvent, GC would not be useful, because of IL's viscosity and high boiling point. Therefore, a method using NMR—another alternative which Dr. Logan's lab had previously explored—was developed. In order to accomplish this, we started by creating a standard ^{1}H NMR sample. First we explored IL **6** and we obtained a ^{1}H NMR spectra of IL **6** in CDCl$_3$ (SAD7A, Table 6), then IL **6** with both 4-chloroanisole and anisole (SAD7B, Table 6).

Table 6:NMR standards, imidazolium IL and 4-chloroanisole/anisole in CDCl3

Reference	Intl. comp.	Temp ℃	Solvent	Analysis	Misc. info
SAD7A	**6**[a]	25	CDCl$_3$	NMR	Standard
SAD7B	**6**[a], **3, 2**	25	CDCl$_3$	NMR	Standard

[a]*IL **6**:1-ethyl-3-methylimidazolium bis(trifluoromethylsulfonyl)imide.*

In SAD7A, the methoxy region of **3** and **2** overlapped with the methyl substituent of the imidazolium ring of IL**6**, and the aromatic hydrogens of IL **6** overlapped with those of **3** and **2** (Spectrum 1).

Spectrum 1: (SAD7B) 1-ethyl-3-methylimidazolium bis(trifluoromethylsulfonyl)imide in CDCl$_3$ with 4-Chloroanisole and Anisole
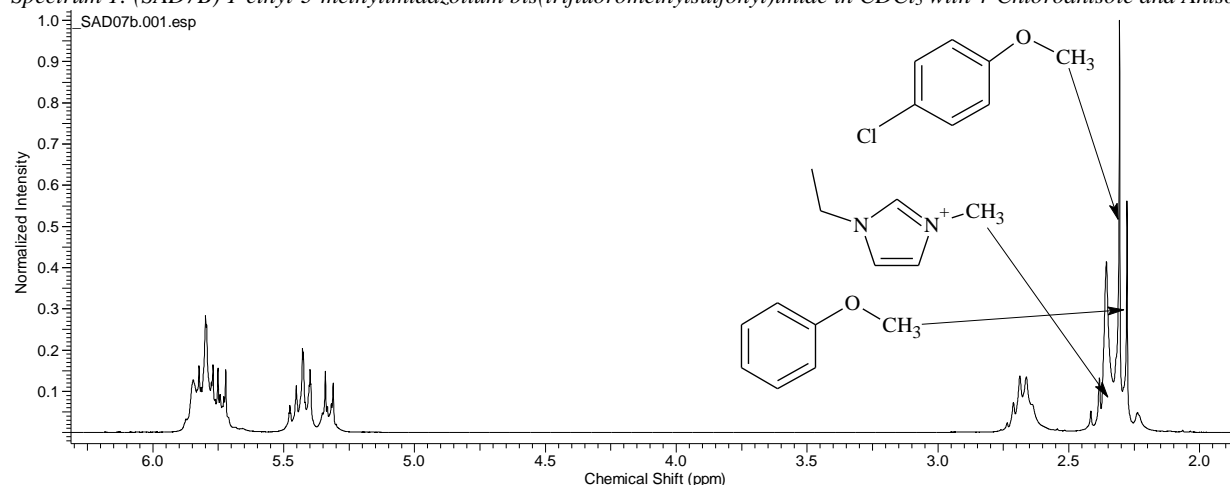
It was also noted at that time that the solution was not very miscible with CDCl₃. Therefore, we tried

dissolving the samples in acetone-d₆, which solved the miscibility issue, and resolved the peaks

(Spectrum 1 vs Spectrum 2).

*Spectrum 2: (JDH6C) 1-Ethyl-3-methylimidazolium bis(trifluoromethylsulfonyl)imide in Acetone with Ligand **5** after 2 Hours*
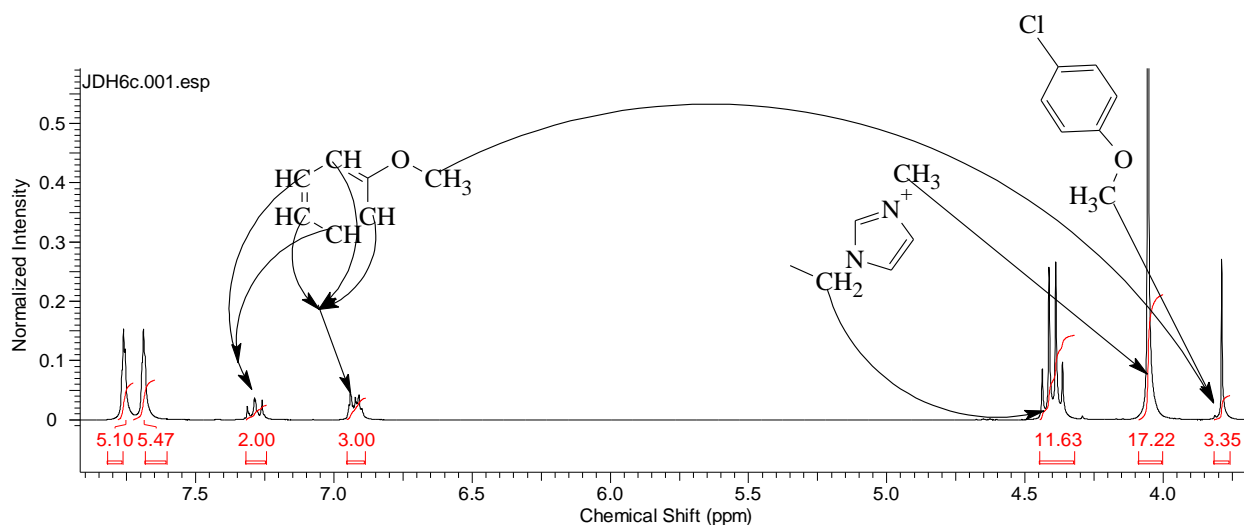
Some spinning sidebands were observed for the methoxy signal around 3.78-ppm; however, this did not alter the results significantly.

However, IL **6** was expensive and in short supply; it was decided to proceed with the trihexyl(tetradecyl)

phosphonium chloride (IL **7a**), which was abundant and inexpensive. Thus, the ILs to be used were the

chloride and bis(trifluoromethylsulfonyl)imide form of the phosphonium IL. Nevertheless, during that

process of discerning the most appropriate analytical technique, Shawn Dirx and I set up **Rxns 3** & **4**

(Table 7). From these reactions in IL **6** both ligands gave reactions that were shown to go to completion,

which gave us the confidence that we were setting up the reactions appropriately. However, determining a

specific rate from these reactions was unreliable because we did not obtain enough time points.

*Table 7: Hydrodechlorination in IL **6** comparing ligands **5** and **4**, NMR performed in Acetone-d₆*

Rxn name		Reference	Ligand	Intl. comp.	Time	Temp ℃	Rxn solv.	Solvent	Analysis	% Conv.
3	H	JDH6A	5	2	00:55	60	6	(CD₃)₂CO	NMR	0
	I	SAD9A	5	2	00:55	60	6	(CD₃)₂CO	NMR	0
	J	JDH6C	5	2	48:00	60	6	(CD₃)₂CO	NMR	90
	K	SAD9C	5	2	48:00	60	6	(CD₃)₂CO	NMR	N/A
4	L	JDH6B	4	2	01:00	60	6	(CD₃)₂CO	NMR	0
	M	SAD9B	4	2	01:00	60	6	(CD₃)₂CO	NMR	N/A
	N	JDH6D	4	2	336:00	60	6	(CD₃)₂CO	NMR	81
	O	SAD9D	4	2	336:00	60	6	(CD₃)₂CO	NMR	100
	P	SAD11A	4	2	336:00	60	6	(CD₃)₂CO	NMR	100
	Q	JDH7A	4	2	336:00	60	6	(CD₃)₂CO	NMR	81

Rxn 3: J *Likely 100 % completion, but the analysis was made difficult by spinning sidebands: observe (Spectrum 2).* **Rxn 3:K** *Evaporated entirely.* **Rxn 4:M** *No data in file.* **Rxn 4: N** *was re-analyzed, after being filtered.* **Rxn 4: O** *was re-analyzed, after being filtered.*

At this point, we wanted to improve the NMR analysis, so, we developed a few more standards (Table 8).

*Table 8:NMR standard samples of **2** & **3** in both chloroform, and acetone*

Reference	Intl. comp.	Temp ℃	Rxn solv.	Solvent	Analysis	Misc. info
Authentic **2** in CDCl₃	3	25	N/A	CDCl₃	NMR	Standard
Authentic **3** in CDCl₃	2	25	N/A	CDCl₃	NMR	Standard
Authentic **2** in (CD₃)₂CO	3	25	N/A	(CD₃)₂CO	NMR	Standard
Authentic **3** in (CD₃)₂CO	2	25	N/A	(CD₃)₂CO	NMR	Standard

The initial method of monitoring the hydrodechlorination via NMR was to compare the methoxy peaks as shown in Spectrum 3 below. Each methoxy peak integrates to 3H if there is a 50:50 mixture in the solution. Therefore, every deviation from 3H:3H reveals the χ (mole fraction) of either compound. Shown in panel **A** (Spectrum 3) are both methoxy peaks from **2**, & **3** integrated together; however, at that point it did not seem useful, because we wanted to compare the relative amounts of either compound. Therefore, we obtained the integration of the two methoxy peaks—often by adjusting the baseline or using curve-fitting to determine an approximation of each contributing peak. Once we determined the two separate integrals, we would divide the integral of compound **2** by the total integration to calculate the mole fraction of **2**: $\frac{\int_2}{\int_2 + \int_3} = \chi_2$. The problem presented by this type of integration—in adjusting the baseline or approximating the area under each peak—was that it was difficult to obtain accurate integrations for the separate methoxy peaks, because they were often overlapping.

Spectrum 3: NMR Analysis—Methoxy Peaks
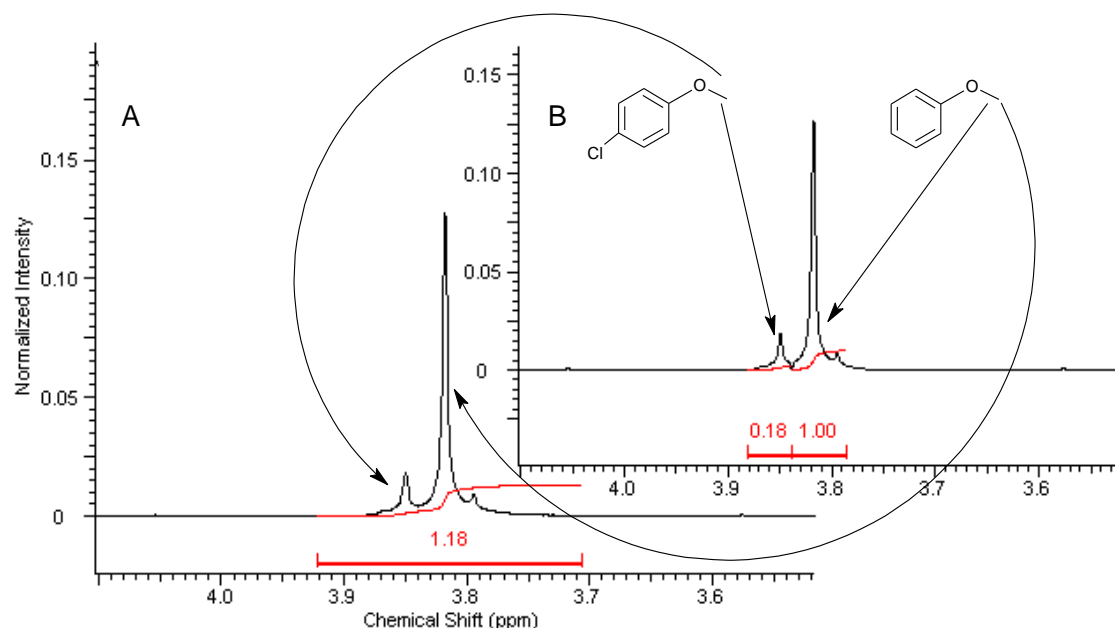
After resolving several spectra, we realized that the anisole compound being produced throughout the reaction was apparent as a transformation of a singlet (3H, 3.75-ppm) from its methoxy signal, and emergence of a doublet of triplets (2H, 6.88 ppm) and a singlet of triplets (1H, 6.91ppm) from its aromatic signals. The 4-chloroanisole had a distinct singlet from the methoxy signal (3H, 3.77-ppm) that usually overlapped with the anisole singlet (3H, 3.75-ppm); essentially this region from 3.6-4.0-ppm represented the total anisole and 4-chloroanisole present. Additionally, three of the anisole aromatic hydrogens were represented by signals in the range between 6.8-7-ppm. Therefore, that aromatic region (3H, 6.8-7-ppm) was divided by the 'consistent' singlet (3H of both compounds, 3.6-4-ppm,), to provide an estimate of the reaction's progress:$\left(\frac{\int_2 (anisole)}{\int_2 + \int_3 (Total\ Reaction)} \cdot 100 = \%\ anisole\ created\ from\ total \right)$.

3. Initial Phosphonium Ionic Liquid (IL) Experiments

Equipped with a more accurate and efficient analytical method, we could run NMR spectra and interpret them much faster. At this point, two experiments were run with ligands **4** and **5** in phosphonium bis(trifluoromethylsulfonyl)imide (IL **7b**) as the solvent at 70 °C (**R$_{xn}$ 5 & 6**), with samples collected after ½ hour, 2 hours, and 48 hours sequentially. IL **7b** was prepared using a simple metathesis[47] (Scheme11) and described in Experimental 9.

*Scheme 11: Metathesis Reaction of Lithium bis(trifluoromethanesulfonyl) imide with IL **7a***
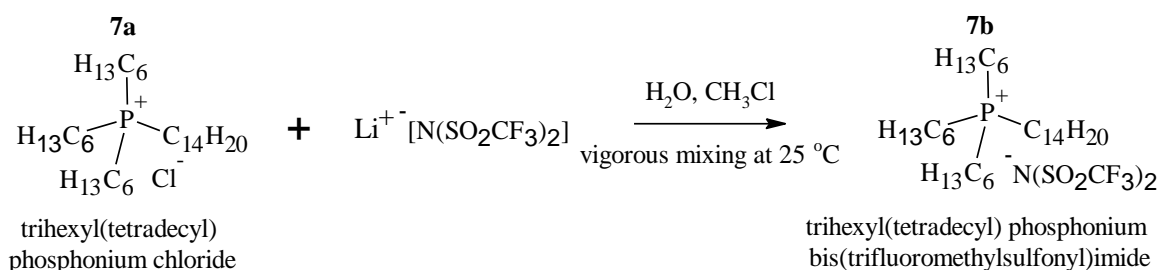
After NMR analysis of **R$_{xn}$ 5 & 6**, it seemed as though ligand **5** was altogether ineffective, as **Rxn 6** with **5** only went to 10% in 48 hours, and **Rxn 5** with **4** went to 95 % (Table 9).

*Table 9: Hydrodechlorination in IL **7b** comparing ligands **4 & 5**, NMR dissolved in chloroform*

R$_{xn}$ name		Reference	Ligand	Intl. comp.	Time	Temp °C	Rxn solv.	Solvent	Analysis	% Conv.
	R	JDH8A	4	2	00:30	70	**7b**	CDCl$_3$	NMR	1
5	S	JDH8B	4	2	02:00	70	**7b**	CDCl$_3$	NMR	4
	T	JDH8C	4	2	48:00	70	**7b**	CDCl$_3$	NMR	95
	U	SAD11B	5	2	00:30	70	**7b**	CDCl$_3$	NMR	0
6	V	SAD11C	5	2	02:00	70	**7b**	CDCl$_3$	NMR	1
	W	SAD11D	5	2	48:00	70	**7b**	CDCl$_3$	NMR	10

However, that was only one experiment and it was recognized that several more trials were necessary to be certain of the results. Nevertheless, the data—both numerical and qualitative—were used to continue evolving both the experimental logistics, and the analytical methods. With the current data set, and Charbonneau's previous observations, it was important that there were no confounding factors such as, water being present and possibly impacting the catalyst; reactant/product evaporation; inconsistent catalyst activation times; or Cl-Pd interaction competing with formate-Pd interaction.

The first confounding factor that we investigated was the possibility of the presence of water affecting the reaction.

4. Investigating the Water Concentration of Ionic Liquid

We decided to test the water content of each ionic liquid (IL) to determine if the more hygroscopic nature of **7a** was influencing the reaction. Between doing an NMR evaluation of each IL's water content—as shown in Ghandi, et al.,[48]—and using Karl Fischer titration, the titration method seemed the simplest and most efficient. However, due to the viscous nature of the IL, we had no simple way to test it neat; therefore, as stated in Experimental 2, a 10% solution of each IL in methanol was made, while testing methanol as well, to control for water introduced by that solvent. Initially, the solutions were made in 5 mL vials, and the methanol tested from a stock bottle. However, there were complications with the methanol increasing in water concentration rapidly—which was due to having the bottle open during testing, and the hygroscopic nature of methanol. These complications led to the use of methanol from an AcroSeal bottle and using a small 0.5 mL vial that was equipped with a septum and evacuated then flushed with argon, to test the IL-methanol mixture. Based on the initial moisture assessments shown in Table 10, if the average ppm H_2O of both samples of **7a** are averaged, the total ppm is 13,440, which is a slightly higher concentration than the **7b** (11,000-ppm). However, it was realized later (discussed in results and discussion section 8) that the average ppm of each IL was inconsistent with the trend of the χ_{H_2O}. The χ_{H_2O} in **7b** (0.33) is 0.065 greater than the average χ_{H_2O} in **7a** (0.265). Because this was not realized until there was NMR analysis of water content, we made the preliminary conclusion that **7a** had a greater water content, and used that conclusion to aid in which experiments to perform. Additionally, after obtaining these results, the plan was to heat the ILs, under vacuum, to control the water content.

Table 10: Karl Fischer titration (KF1) as shown in Experimental 2

Sample composition	Mean (S)	St. Dev. (S)	% dev S	Avg ppm H_2O	χ_{H_2O}
CH_3OH	671.2	146.5	21.8%	670	0.0012
9.3% **7b** in CH_3OH	1670.5	360.7	21.6%	11000	0.33
16.9% **7a** in CH_3OH	1688.3	152.1	9.0%	6700	0.16
8.0 % **7a** in CH_3OH	2241.6	479.2	21.4%	20200	0.37

*The above ILs were used, as is, in all reactions—until **Rxn 28** (results and discussion section 8, Table 22)—and were not heated under vacuum prior to use until after that experiment.*

5. Determining the Best Reaction Temperature

Eventually we planned to heat the ILs under vacuum to remove H_2O. However—even if the water content

was solved, running back-to-back experiments in IL that took 8 hours to complete was impractical, given

that one of the goals was to determine whether a second equivalent of aryl chloride after reaction

completion would react faster in IL than in methanol. Therefore, we ran a few experiments to find the best

temperature. Initially we ran reactions **7** and **8** (Table 11) at 70℃ as before, with the premise that there

may have been some experimental errors in **5** and **6**; however, the reactions were not producing anything

for the first four hours; therefore the temperature was increased to 80℃, and there was an obvious

increase in catalytic activity.

*Table 11: Hydrodechlorination in IL **7b** comparing ligands **4** & **5**, while adjusting temperature, NMR dissolved in chloroform*

R_{xn} name		Reference	Ligand	Intl. comp.	Time	Temp ℃	Rxn solv.	Solvent	Analysis	% Conv.
7	X	JDH13(1a)	5	2	00:30	75	**7b**	CDCl₃	NMR	0.64
	Y	JDH13(1c)	5	2	01:40	75	**7b**	CDCl₃	NMR	2.13
	Z	JDH13(1g)	5	2	03:40	75	**7b**	CDCl₃	NMR	3.49
	A	JDH13(1h)	5	2	05:10	80	**7b**	CDCl₃	NMR	19.92
	B	JDH13(1i)	5	2	24:00	80	**7b**	CDCl₃	NMR	95.57
8	C	JDH13(2a)	4	2	00:30	75	**7b**	CDCl₃	NMR	1.04
	D	JDH13(2c)	4	2	01:40	75	**7b**	CDCl₃	NMR	2.55
	F	JDH13(2g)	4	2	03:40	75	**7b**	CDCl₃	NMR	8.39
	G	JDH13(2h)	4	2	05:10	80	**7b**	CDCl₃	NMR	20.66
	H	JDH13(2i)	4	2	24:00	80	**7b**	CDCl₃	NMR	N/A[a]

[a] Spectral data was missing any semblance of 4-chloroanisole or anisole, likely entirely evaporated. This issue might have been solved using a mini column and GC like the methods discussed in results and discussion section 6. However, that analysis was too time consuming.

After performing these reactions, we decided to test IL **7a** at 80℃ and determined that 80℃ was a good

temperature to run the reactions. From **Rxns 9** and **10** (Table 12), we were able to test adding another

equivalent of **2**; however, at 80℃ the reaction did not seem to be proceeding, and the temperature was

increased to 85℃. Additionally, due to the slow initiation, the second equivalent of **2** was added the

following day. The problem with this process is that the catalyst would often settle as palladium black,

or—as we discovered later (see results and discussion sections 7, and 8)—both 4-chloroanisole and

anisole were evaporating, and there was no way to assess whether the reaction ran to completion.

Nevertheless, it revealed that the catalyst from ligand **4** was still active while ligand **5** had, which

confirmed Zdanowski's work in methanol (Figure 4).

*Table 12: Hydrodechlorination in IL **7a** comparing ligands **4 & 5, while adjusting temperature**, NMR dissolved in chloroform*

R_{xn} name		Reference	Ligand	Intl. comp.	Time	Temp ℃	Rxn solv.	Solvent	Analysis	% Conv.
9	*I*	JDH15(1a)	**5**	**2**	00:55	80	**7a**	CDCl$_3$	NMR	1.35
	J	JDH15(1b)	**5**	**2**	01:40	80	**7a**	CDCl$_3$	NMR	2.52
	K	JDH15(1c)	**5**	**2**	02:10	85	**7a**	CDCl$_3$	NMR	9.40
	L	JDH15(1d)	**5**	**2**	02:40	85	**7a**	CDCl$_3$	NMR	11.83
	M	JDH15(1e)	**5**	**2**	03:10	85	**7a**	CDCl$_3$	NMR	14.34
	N	JDH15(1f)	**5**	**2**	21:00	85	**7a**	CDCl$_3$	NMR	93.10
	O	JDH15(1g)	**5**	**2**	27:45	85	**7a**	CDCl$_3$	NMR	0.00^a
	P	JDH15(1h)	**5**	**2**	28:55	85	**7a**	CDCl$_3$	NMR	0.00
	Q	JDH15(1i)	**5**	**2**	44:55	85	**7a**	CDCl$_3$	NMR	N/A^b
10	*R*	JDH15(2a)	**4**	**2**	00:55	80	**7a**	CDCl$_3$	NMR	0.74
	S	JDH15(2b)	**4**	**2**	01:40	80	**7a**	CDCl$_3$	NMR	4.75
	T	JDH15(2c)	**4**	**2**	02:10	85	**7a**	CDCl$_3$	NMR	7.68
	U	JDH15(2d)	**4**	**2**	02:40	85	**7a**	CDCl$_3$	NMR	N/A
	V	JDH15(2e)	**4**	**2**	03:10	85	**7a**	CDCl$_3$	NMR	9.16
	W	JDH15(2f)	**4**	**2**	21:00	85	**7a**	CDCl$_3$	NMR	94.36
	X	JDH15(2g)	**4**	**2**	27:45	85	**7a**	CDCl$_3$	NMR	1-2%^{c}
	Y	JDH15(2h)	**4**	**2**	28:55	85	**7a**	CDCl$_3$	NMR	10%
	Z	JDH15(2i)	**4**	**2**	44:55	85	**7a**	CDCl$_3$	NMR	20-30%

^{a} *JDH15(1g) 1.25 hr after second equivalent added (immediate should have been 50:50 anisole to 4-chloroanisole). However, after standardizing to IL peaks, we found that the sample of 4-chloroanisole was evaporating, only 55% of original sample yielded due to evaporation.* ($\frac{\% \, to \, IL \, final}{\% \, to \, IL \, inital} * percent \, conversion$). ^{b} *Sample evaporated and NMR was not useful to analyze .^{c} JDH15(2g) 1.25 hr after second equivalent added, evaporation was note. Due to interpretation difficulties, only an approximate range can be reported..*

6. Exploring Other Avenues of Reaction Analysis

In the process of discovering the tentative result that ligand **4** formed a catalyst having a longer lifetime than the one from ligand **5**, there was much difficulty when interpreting the NMR spectra after the second addition of 4-chloroanisole. For example, **Rxn 9: N** (Table 12), a second addition of 4-chloroanisole was added 1.5 hours prior to sampling (**Rxn 9: O**, Table 12) and there was evaporation of the product in the vessel that it was added to. Therefore, when assessing the NMR of **Rxn 9: O** there was not a 50:50 ratio of anisole to 4-chloroanisole—if 93% of the original sample was still in the vessel at the time of addition, then the ratio of anisole at 1.5 hours would likely have been 60:40, the ratio was more 40:60 (Spectrum 4). At this point, we had not identified that there was a sample evaporation problem, and this led to pursuing several alternative explanations.

Spectrum 4: NMR of IL 7a, and Ligand 4, 1.25 Hours after Second Addition
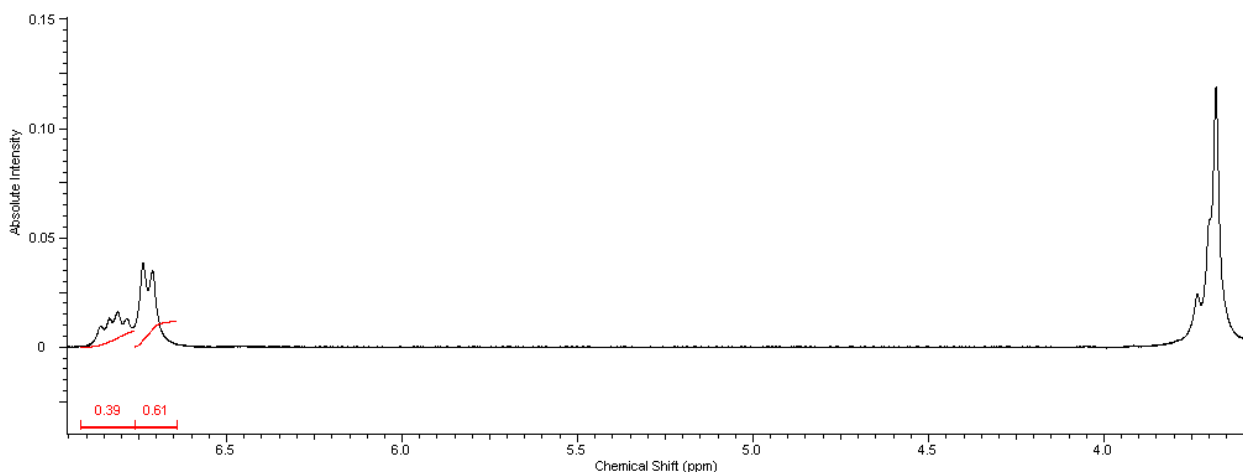
First, because the NMR was poorly resolved, the difference might be explained as a poorly shimmed sample or solvent interactions that distorted the spectrum. Second, the IL may have been decomposing and causing side reactions. Third, the NMR data analysis might have all been less accurate and precise than GC data, and GC might be preferred to follow reactions. Finally, there may have been evaporation of anisole before adding the second equivalent. We decided to test the first three hypotheses using column chromatography to separate the compounds and GC to analyze them, given that the IL could be separated from the anisole and 4-chloroanisole. This would be confirmed with TLC, KMnO$_4$, and NMR as

explained in Experimental 7. The experimental results below show that fractions JDH 17 (1a) and (2a)—using 70-230 mesh, 63-200 μm particle size silica gel for the column—had IL in them, wherein we decided to make a shorter column (to reduce the time of elution) with 230-400 mesh size, 40-63 μm particle size silica gel. The eluate collected from the reagent grade silica did not seem to contain any IL, because a distinct band that seemed to represent the IL did not move; however, TLC results showed that the sample had a small spot that did not migrate with the UV active compound, suggestive of IL. At this point, we used NMR to analyze the sample, which revealed signals suggestive of IL; however, one of the peaks normally attributed to the IL was missing (Spectrum 5). Therefore an NMR of the 99:1 C_6H_{12}:CH_2Cl_2 loading solvent was run to rule out any impurities; this NMR did not have any impurities and seemed to confirm the presence of alkenes in the eluate (Spectrum 5).

Spectrum 5: Eluate from Column Chromatography Analyzed via NMR
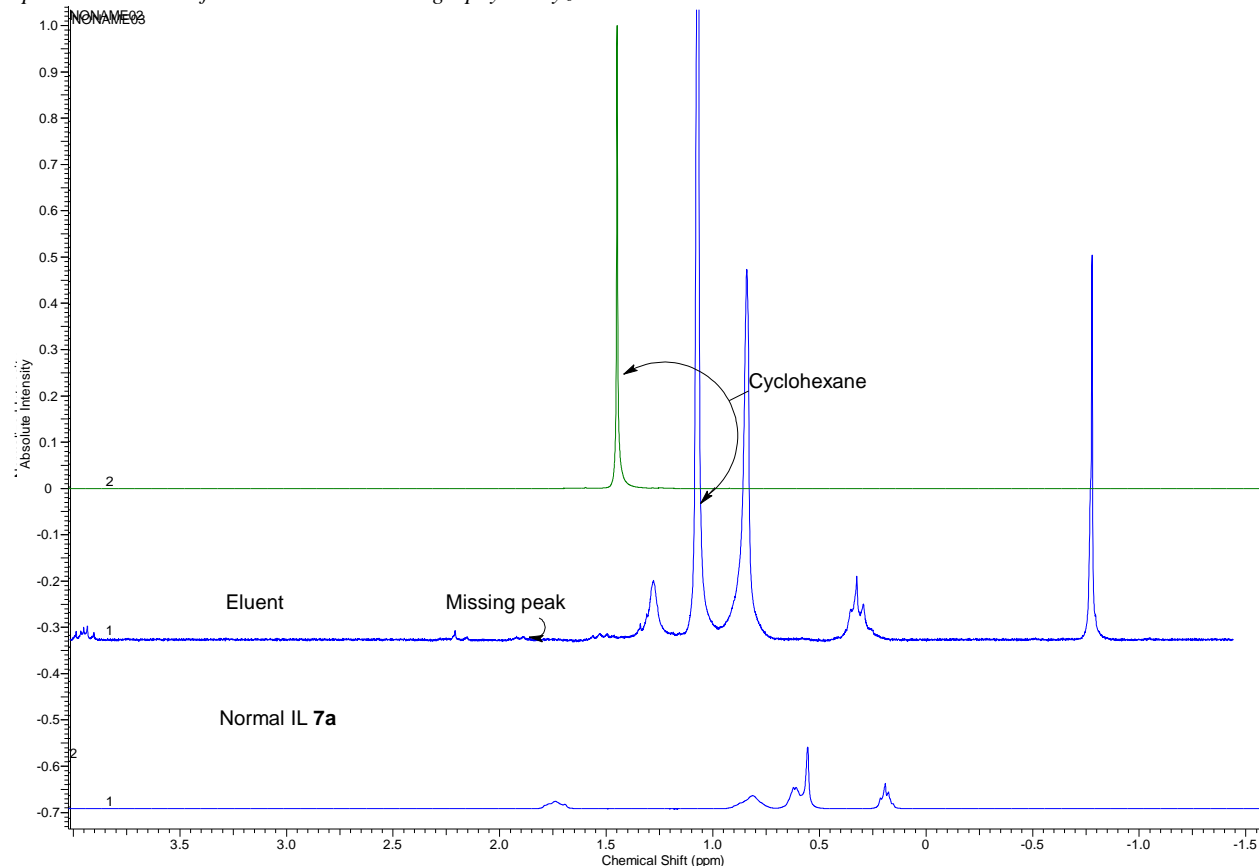
This is when we decided to use KMnO₄ as a Baeyer's reagent to stain a TLC plate as described in Experimental 7. The results of the experiment revealed that the Baeyer's reagent primarily interacted with—a large spot as show in Figure 6 drawn after the experiment—also suggesting that there were alkenes present in the IL. Despite the result, it was still inconclusive regarding the presence of phosphines from a beta elimination involving the phosphonium IL. Further studies such as phosphorus NMR are possible, and are being pursued by other students at this time.

Table 13: Column Chromatography, TLC, and Baeyer's Reagent Results

Reference	Intl. comp.	Rxn solv.	Solvent	Analysis	
JDH17(1a)	**3, 2**	**7a**	CDCl₃	NMR/TLC	pos. for IL
JDH17(2a)	**3, 2**	**7a**	CDCl₃	NMR/TLC	pos. for IL
JD18(1a)	**3, 2**	**7a**	CDCl₃	NMR/TLC	pos. for alkenes
Authentic 99:1 **C₆H₁₂:CH₂Cl₂** in CDCl₃	**C₆H₁₂:CH₂Cl₂**	**N/A**	CDCl₃	NMR	Standard

Figure 6 TLC, Baeyer's reagent results
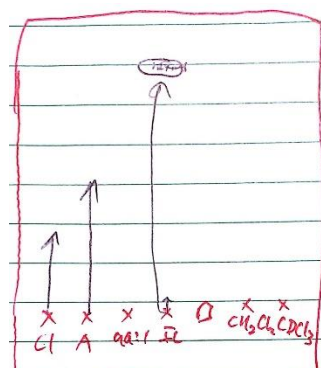
4-chloroanisole with an Rf of roughly .45, anisole at .55, and the IL had movement to .85, as well as .05. With the Baeyer's reagent, there was coloration of a brown band as circled in the diagram, suggesting the presence of alkenes.

After believing that we had developed a method of separating the IL from the other compounds, we started 2 reactions that we planned to analyze with GC, **Rxn 12**, and **Rxn 13** (Table 14). However, the process of separating the IL and developing neat samples with the worry that anisole and 4-chloroanisole were not coming off the column at similar times, made the extraction/analysis too time consuming, and the experiment was discontinued. However, we decided to spend the time collecting one sample for GC from **Rxn 13** (Table 14) at 22.5 hours, shown as **Rxn 14: U** (Table 14), and four other samples of that reaction were placed in differing solvents and analyzed using NMR. The results in the table below show that DMSO-d₆ had a significant interaction with the reactants and products that distorted the spectra, leading to an erroneous 13.46% for **Rxn 12** at 22.5 hours**,** and 8.13% for **Rxn 13** at 22.5 hours. Besides eliminating the potential the use of DMSO-d₆, the experiment revealed that NMR data from running in either CDCl₃ or (CD₃)₂CO, were equally as accurate as GC, and the effort to separate the IL from the other compounds for GC was much greater than deciphering the NMR. Thus for the remainder of the experiments in ILs they were analyzed using NMR. Furthermore, there was the possibility of running the entire reaction in an

NMR tube with a septum (0) thus gathering real-time data, and having no sample collections. In theory, this would provide more realistic data sets and accuracy; however, after pursuing that method, the logistics—mainly caused by the increased pressure from CO_2—prohibited the possibility of running the experiment, thus making the extra preparations such as weighing of miniscule amounts futile. The results of this experiment are shown below (Table 15), with little to no product formation after 3.75 hours.

Table 14: NMR vs GC Analysis for Reactions in ILs

Rxn name		Reference	Ligand	Intl. comp.	Time	Temp ℃	Rxn solv.	Solvent	Analysis	% Conv.
12[a]	D	JDH22(1a)	**4**	**2**	01:00	85	**7a**			
	F	JDH22(1b)	**4**	**2**	02:00	85	**7a**			
	G	JDH22(1c)	**4**	**2**	03:45	85	**7a**			
13[b]	H	JDH22(2a)	**5**	**2**	01:00	85	**7a**			
	I	JDH22(2b)	**5**	**2**	02:00	85	**7a**			
	J	JDH22(2c)	**5**	**2**	03:45	85	**7a**			
14	*Q*	JDH23(2a)	**5**	**2**	22:30	85	**7a**	$CDCl_3$	NMR	45
	R	JDH23(2b)	**5**	**2**	22:30	85	**7a**	$(CD_3)_2CO$	NMR	48
	S	JDH23(2c)	**5**	**2**	22:30	85	**7a**	DMSO	NMR	14
	T	JDH23(2f)	**5**	**2**	22:30	85	**7a**	$CDCl_3$	NMR	44
	U[c]	JDH23(2g)	**5**	**2**	22:30	85	**7a**	CH_3OH	GC	43
15	N	JDH23(1a)	**4**	**2**	22:30	85	**7a**	$CDCl_3$	NMR	17
	O	JDH23(1b)	**4**	**2**	22:30	85	**7a**	$(CD_3)_2CO$	NMR	20
	P	JDH23(1c)	**4**	**2**	22:30	85	**7a**	DMSO	NMR	8

[a] *No samples from this reaction were analyzed using GC because extraction/analysis was too time consuming.* [b,c] *Only one sample from this reaction was analyzed using GC (**Rxn 14:U**).*

Table 15: Monitoring the Hydrodechlorination Reaction in an NMR Tube

Rxn name		Reference	Ligand	Intl. comp.	Time	Temp ℃	Rxn solv.	Solvent	Analysis	% Conv.
16	*K*	JDH22(3a)	**4**	**2**	01:00	85	**7a**	$CDCl_3$	NMR	0
	L	JDH22(3b)	**4**	**2**	02:00	85	**7a**	$CDCl_3$	NMR	3
	M	JDH22(3c)	**4**	**2**	03:45	85	**7a**	$CDCl_3$	NMR	3

7. Suspected Sample Evaporation

After determining that NMR in CDCl$_3$ was the most time effective and sufficiently accurate way to analyze, we decided to run an experiment in IL **7a** to accumulate data with regards to ligand effects, by running one reaction with ligand **4** and the other with **5**. In Table 16 below, **Rxn 17** and **18**, both only ran to 10% within 5 hours. The reaction with ligand **4** (**Rxn 18**) failed to run to completion within 22 hours—of note, the reaction was already changing to a brown color 17 minutes after all reagents were added suggesting quick initiation. However, given the results, that may have been an indication of palladium black forming and the catalyst actually being destroyed by various confounding factors, such as sample evaporation, oxygen contamination, water content, or chloride anion inhibition—most of which were not serious considerations at this time. Therefore, we then ran the same experiment in IL **7b**, which showed that **Rxn 19**, with ligand **5**, went to completion in 3.5 hours, but **Rxn 20** with ligand **4** was only at 48% at that time. Another sample was then collected at 66 hours and 35 minutes, which showed that both reactions had finished, at that point, another equivalent of 4-chloroanisole was added. After letting the reaction run for another hour, a sample was taken but just like **Rxn 9** and **10** the ratio of compound **3:2** was lower than 50:50. At this point, we decided to use the NMR spectra to assess the possibility of sample evaporation.

To assess sample evaporation, we assumed that the IL is not nearly at its boiling point, and remains constant in the reaction. Therefore, if we were to divide the methoxy peak integration like panel A of Spectrum 3 (also shown below)—which represent both the 4-chloroanisole and the anisole—by the summation of IL peak integrations (Spectrum 6), that would be an approximation of the fraction of anisole-4-chloroanisole still in the reaction vessel, allowing us to follow the reaction.

Spectrum 6: JDH27(1)[3] Comparison of IL7b Peaks and Compound 2/3 Methoxy Peaks
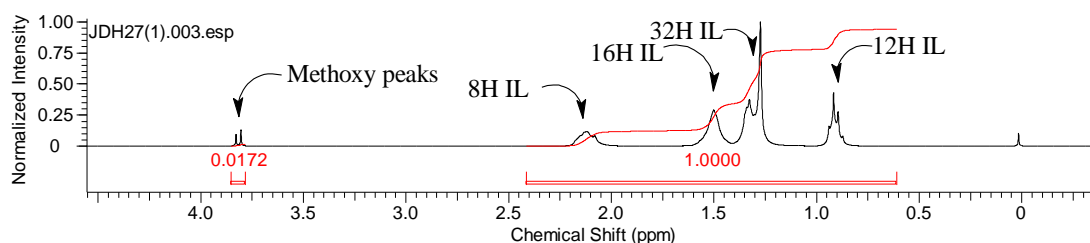
*Table 16: Hydrodechlorination in IL **7a/7b** Comparing Ligands **4/5**, NMR Dissolved in Chloroform*

Rxn name			Reference	Ligand	Intl. comp.	Time	Temp °C	Rxn solv.	Solvent	Analysis	% Conv.	% 3:IL
17	V		JDH25(1a)	5	2	00:35	81	7a	CDCl$_3$	NMR	0	
	W		JDH25(1b)	5	2	01:07	82	7a	CDCl$_3$	NMR	0	
	X		JDH25(1c)	5	2	01:32	82	7a	CDCl$_3$	NMR	2	
	Y		JDH25(1d)	5	2	02:00	82	7a	CDCl$_3$	NMR	3	
	Z		JDH25(1e)	5	2	02:30	81	7a	CDCl$_3$	NMR	4	
	A		JDH25(1f)	5	2	03:30	82.5	7a	CDCl$_3$	NMR	6	
	B		JDH25(1g)	5	2	04:00	82	7a	CDCl$_3$	NMR	7	
	C		JDH25(1h)	5	2	04:30	82	7a	CDCl$_3$	NMR	9	
	D		JDH25(1i)	5	2	05:25	82	7a	CDCl$_3$	NMR	10	
	F		JDH25(1j)	5	2	22:25	82.5	7a	CDCl$_3$	NMR	95	
18	G		JDH25(2a)	4	2	00:35	81	7a	CDCl$_3$	NMR	0	2.24
	H		JDH25(2b)	4	2	01:07	82	7a	CDCl$_3$	NMR	0	1.95
	I		JDH25(2c)	4	2	01:32	82	7a	CDCl$_3$	NMR	0	2.04
	J		JDH25(2d)	4	2	02:00	82	7a	CDCl$_3$	NMR	0	1.95
	K		JDH25(2e)	4	2	02:30	81	7a	CDCl$_3$	NMR	2	1.55
	L		JDH25(2f)	4	2	03:30	82.5	7a	CDCl$_3$	NMR	4	1.50
	M		JDH25(2g)	4	2	04:00	82	7a	CDCl$_3$	NMR	7	1.50
	N		JDH25(2h)	4	2	04:30	82	7a	CDCl$_3$	NMR	7	1.50
	O		JDH25(2i)	4	2	05:25	82	7a	CDCl$_3$	NMR	8	1.27
	P		JDH25(2j)	4	2	22:25	82.5	7a	CDCl$_3$	NMR	14	0.86
19	Q	1	JDH27(1)	5	2	00:45	≈ 84[a]	7b	CDCl$_3$	NMR	13	2.03
	R	2		5	2	01:30	83.5	7b	CDCl$_3$	NMR	24	2.84
	S	3		5	2	02:30	83	7b	CDCl$_3$	NMR	41	1.79
	T	4		5	2	03:20	82.5	7b	CDCl$_3$	NMR	90	1.34
	U	5		5	2	66:35	82	7b	CDCl$_3$	NMR	95	1.20
	V	6		5	2	67:45	81	7b	CDCl$_3$	NMR	0-10[c]	2.51
	W	7		5	2	69:45	82	7b	CDCl$_3$	NMR	0-10[c]	2.36
	X	8		5	2	89:45	82	7b	CDCl$_3$	NMR	N/A	N/A
20	Y	1	JDH27(2)	4	2	00:45	≈ 84[b]	7b	CDCl$_3$	NMR	1	2.22
	Z	2		4	2	01:30	83.5	7b	CDCl$_3$	NMR	11	2.15
	A	3		4	2	02:30	83	7b	CDCl$_3$	NMR	32	1.68
	B	4		4	2	03:20	82.5	7b	CDCl$_3$	NMR	48	1.53
	C	5		4	2	66:35	82	7b	CDCl$_3$	NMR	94	1.20
	D	6		4	2	67:45	81	7b	CDCl$_3$	NMR	0-10[c]	3.14
	F	7		4	2	69:45	82	7b	CDCl$_3$	NMR	0-10[c]	3.04
	G	8		4	2	89:45	82	7b	CDCl$_3$	NMR	0-10[c]	2.30

[a,b] *Bath was set to 180 ℃ accidentally for 30 mins, may have reached 90 ℃; however, bath turned down after 30 mins to 175 ℃, and reached 84 ℃ in 15 min..[c] Could not determine the exact ‰ of anisole due to complications with evaporation, and not sampling directly when the 4-chloroanisole was added.*

In the process of optimizing this analysis it was found that evaporation rates could be established for the reaction—despite large time gaps between sampling and greater evaporation during sampling—by following the fraction of anisole-4-chloroanisole lost over a given time period. However, this was not recognized until later, as unexpected peaks in the spectra complicated the initial assessments. Often times, water in the NMR spectrum appears as a broad band beneath the IL, and it would seem as though the

fraction of anisole(**3**)-4-chloroanisole(**2**) was minimal. Then the next NMR—without water disrupting the spectrum—would make it seem as though the sample was not evaporating. Additionally, we were worried that the anisole(**3**) or 4-chloroanisole(**2**) might be evaporating at different rates. Therefore, we ran an experiment to test the evaporation of each compound. We set up an experiment with a 1:1 ratio (1 mmol:1 mmol) of anisole(**3**) to 4-chloroanisole(**2**), in IL**7a**, and began sampling. Initially, while only evaluating the % of anisole(**3**) in the reaction, and % of the anisole(**3**)-4-chloroanisole(**2**) to the IL we believed that the results were inconclusive, especially since the sample taken at 4.5 hours was poorly resolved (Table 17, Spectrum 7). However, it seemed safe to conclude that both compounds were evaporating, but it was not obvious which was evaporating faster. After further analysis, and determining the percentage of **3**, percentage of **3** to IL, percentage of **2** to IL, and percentage of both to IL, it seems clear that the sample at 4.5 hours is erroneous due to the distorted spectrum. In addition, the sample at 00:00 is likely inaccurate because of the viscous nature of the IL and it was not ensured that all the materials had been properly mixed before sampling.

*Table 17: Evaporation of a 1:1 mixture of **2**:**3** in IL **7a** at 85℃*

Rxn name	Reference		Time	Temp ℃	Rxn solv.	Solvent	Analysis	%of 3	%3 to IL	%2 to IL	% to IL	ppm H_2O
	A	1	00:00	85	**7a**	$CDCl_3$	NMR	62.78	6.317	3.405	10.14	64
	B	2	02:00	85	**7a**	$CDCl_3$	NMR	35.14	0.173	0.290	0.510	64
35	C	3	04:30	85	**7a**	$CDCl_3$	NMR	4.48	0.013	0.165	0.187	64
	D	4	06:35	85	**7a**	$CDCl_3$	NMR	12.47	0.023	0.299	0.190	64
	F	5	360:00	85	**7a**	$CDCl_3$	NMR	4.66	0.014	0.176	0.197	64

Rxn 35: *C was a poorly shimmed and resolved spectrum.*

Excluding samples 1 and 3, as shown in Figure 7 below, the results suggest that the best hypothesis would be that the anisole is evaporating faster, and only when it is entirely gone, does the 4-chloroanisole actually begin to evaporate. However, this needs to be explored further. Thus, the only thing this experiment shows is that both 4-chloroanisole and anisole are evaporating. Additionally, these results forced us to develop a new method of sampling the reactions; we began attaching a septum to the Wiretrol disposable pipet, and lowering the flow of argon when sampling.

*Figure 7: Evaporation of a 1:1 mixture of **2:3** in IL **7a** at 85℃ (excluding samples 1 and 3)*
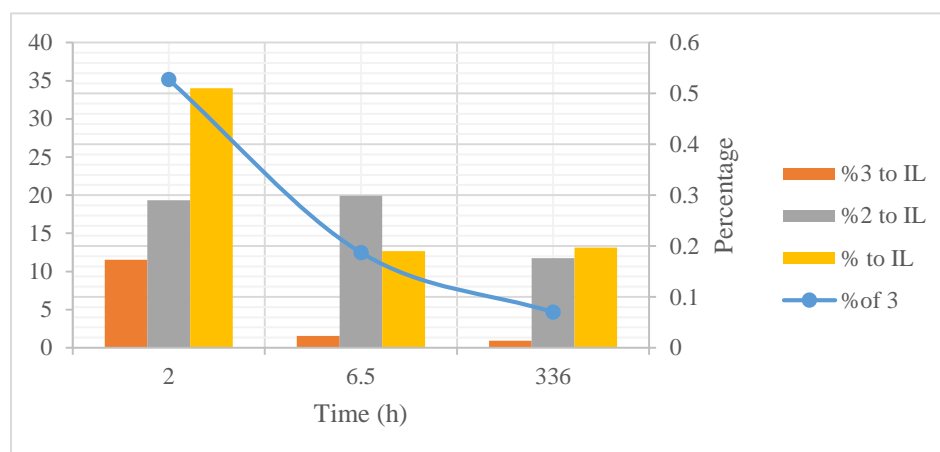
Spectrum 7: Evaporation of a 1:1 Mixture of 2:3 in IL 7a at 85℃
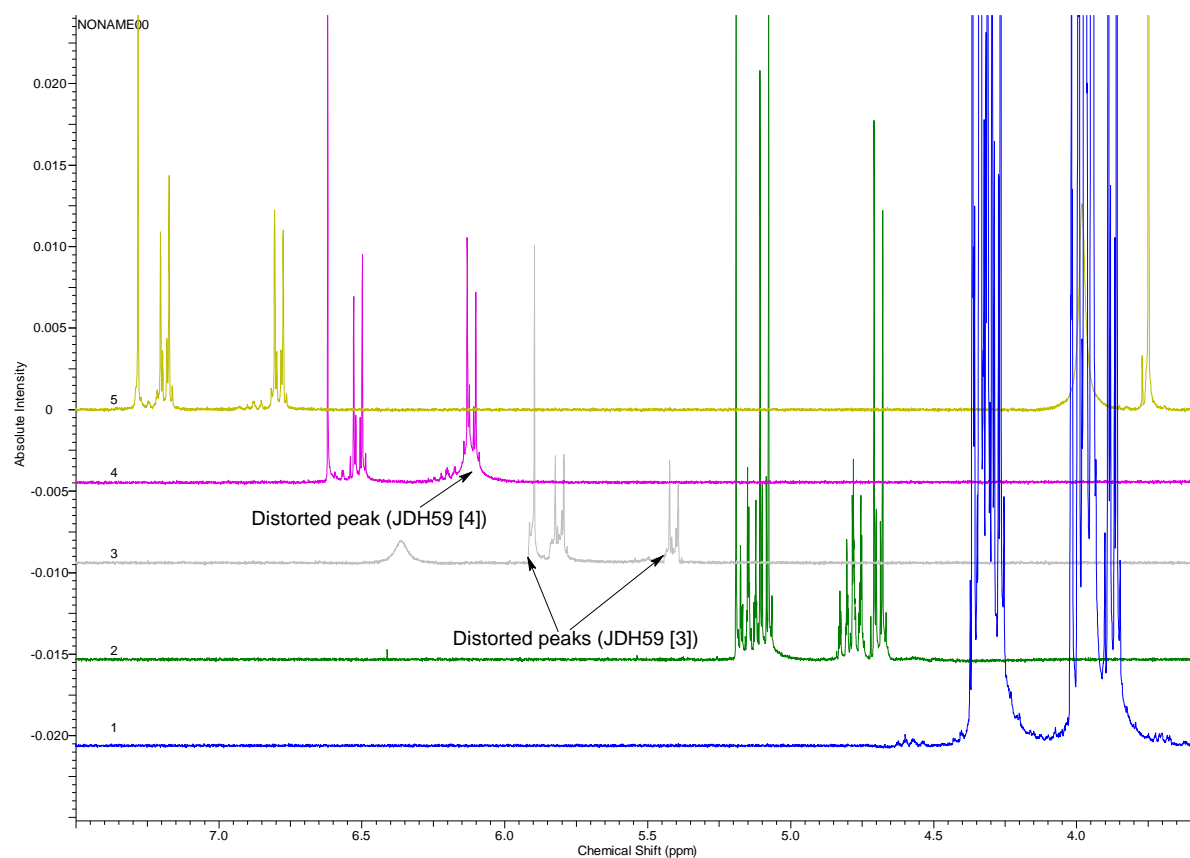
8. Water Content Analysis, and Controlling Initiation Times

While analyzing the possibility of evaporation we also began analyzing the water content of each IL, because up to this point reactions in IL **7b** were faster than **7a**, and there were only two appreciable differences between IL **7a** and **7b**; water content, and anion character. IL **7b**, based on preliminary analysis, was assumed to be less hygroscopic with a water content of 11,393-ppm vs 13,440-ppm. In fact, at that time we were suspicious that it was much less hygroscopic, and were worried that the Karl Fischer with 10% solutions in methanol was too inaccurate due to water possibly being introduced from the methanol. Therefore, we planned to, analyze the water content using NMR, and then remove the water from both ILs (by heating them under vacuum), so that the both of them have the same (low) amount of H_2O. Two samples were prepared, one for each IL (that had not been heated under vacuum yet), containing 50 uL of the IL and 0.6 mL of $CDCl_3$. Then the solution was assessed at 25 °C using NMR. From the initial assessment it was difficult to discern where the actual water peak was. Initially we looked to Gottlieb, et al., 1997, which suggests a chemical shift of 1.56-ppm for water in $CDCl_3$.[49] However, with TMS as a reference, it seemed as though the only peak likely to represent H_2O was between 2.25-ppm and 4.0-ppm (Spectrum 8). Ghandi et al., 2008 have reported that the interactions of water with IL**7a** can be observed via NMR, and as those interactions change, the water will shift on the spectrum.[48] Therefore, to confirm that this peak was indeed water, we planned to spike the sample with D_2O and exchange the protons of the water in the sample, thereby allowing the water to shift further downfield or upfield due to a different interaction with the solvent. Spectrum 9 shows the results of this experiment with the well resolved water peak at 2.56-ppm. After determining that the broad peak visualized between 2.25-ppm and 4.0-ppm was indeed from water, it was integrated as well as one of the peaks attributed to the IL. Then each integration was divided by the respective number of hydrogens that they represent to give the moles of that material in the sample $\left(\dfrac{integration\ (mol\ H)}{\frac{2\ mol\ H}{1\ mol\ H_2O}} = mol\ H_2O \right)$ and $\left(\dfrac{integration\ (mol\ H)}{\frac{8\ mol\ H}{1\ mol\ IL}} = mol\ IL \right)$. Then χ_{H_2O}

of each IL were calculated by dividing the moles of water by the total moles of sample $\left(\frac{moles\ H_2O}{moles\ IL + H_2O} = \right.$

$\left. \chi_{H_2O} \right)$ giving a χ_{H_2O} of 0.444 in IL **7a** and 0.037 in IL **7b** (Table 18).

Then we converted the earlier Karl Fischer results to χ_{H_2O} and realized that they were entirely

contradictory to the results from the NMR, suggesting a χ_{H_2O} of 0.265 in **7a** and 0.33 in **7b** (Table 10).

*Spectrum 8: IL **7a** and **7b** NMR Analysis of Water Content*
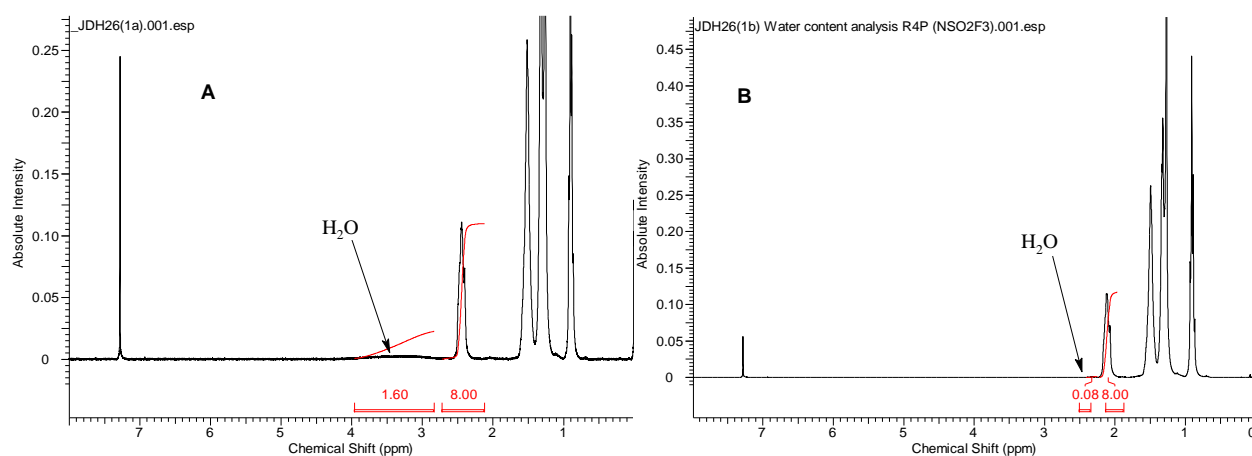
*Spectrum 9: IL **7a** with 30 µL D₂O in CDCl₃*
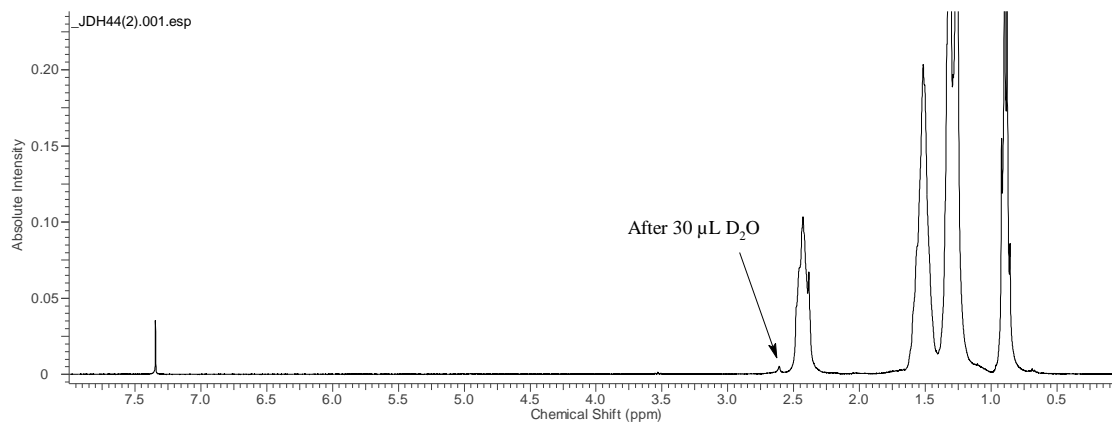
Table 18: NMR Analysis of Water Content

Sample composition	ppm H₂O	χ_{H_2O}
NMR **7a** in CDCl₃	27729	0.444
NMR **7b** in CDCl₃	908	0.037

After running a few more Karl Fischer experiments with 10% solutions of IL, it became apparent that

extended exposure of the needle to room air correlated to a higher reading on the Karl Fischer titrator.

Therefore, it was likely that many of the Karl Fischer experiments were not accurate, and so we sought to

improve the analysis. However, those Karl Fischer experiments seemed to coincide with the NMR results that IL **7a** did have a significantly higher χ_{H_2O}, averaging 0.122 with a deviation of 7.6%.

*Table 19: Second Set of Karl Fischer Titrations of IL **7a** and **7b***

Reference	Sample composition	St. Dev. (S)	Mean (S)	% dev S	Avg ppm H₂O	χ_{H_2O}
JDH 29[a]	CH₃OH	47.8	252.3	18.9%	252.3	0.007
JDH 29	9.1% **7a** in CH₃OH	51.0	668.9	7.6%	4835.3	0.122
JDH 38[b]	10.0% **7b** in CH₃OH	72.7	234.6	31.0%	76.1	0.003

[a] *Samples of CH₃OH that had been exposed to air for too long were excluded.* [b] *Samples of the first batch of 7b before consistently heating under vacuum*

After establishing that **7a** had an appreciable amount of water compared to **7b**, we ran an experiment comparing **Rxn's 21** & **23** (both in IL **7b**)—that had an added 40 μL of water (giving a total χ_{H_2O} of 0.44)—to a control (**Rxn 22**, also in IL **7b**) with no added water (Figure 8). From this experiment, we planned to begin testing the hypothesis that reactions in IL would run slower if they had a higher water concentration. Therefore, we also compared these reactions in **7b**, with added water, to average rates of reactions in **7a**. In order to discern reliable trends from the reactions, samples taken while the reactions were proceeding were used to determine the % conversion/hr. Figure 8 below shows the trends that we were seeing from the data at this time. Overall, it seemed clear that reactions in **7b** (that on average had less water) ran faster, and that reactions with ligand **5** compared to reactions with ligand **4** were also faster; however, the biggest impact seemed to be from the IL, with rates of 10.38%/hour in **7b** vs 3.3%/hour in **7a**. Additionally from **Rxns 21-23** it seemed that water also slowed the reaction.

*Figure 8: Rate Analysis of **Rxns 5-23** and Impact of Mole Fraction of H₂O on IL **7b***
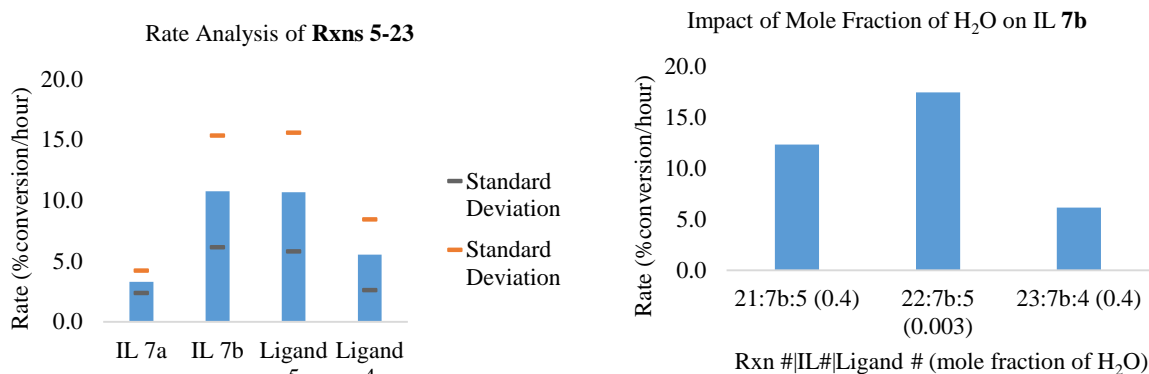
*The bottom axis contains the information of the reaction rate represented by that column by stating the Rxn number, character of the IL, and finally the ligand, In this figure each reaction from **5** to **23** are compared using the rate in %completion /hour, the rates were standardized by excluding samples well beyond the time period appropriate for sampling.*

From these experiments, it seemed that water was having a significant impact on the reaction. However, at this same time, we began running out of IL **7b**; therefore, we made another batch of IL **7b** as in Experimental 9. To ensure that the IL that we prepared was usable for reactions we needed to assess its purity via NMR, looking for CDCl₃. Therefore, we prepared several standards, and analyzed the IL in DMSO concluding that it had residual CDCl₃, as shown in Table 20 and Spectrum 10.

*Table 20: Standards and Sample for Analysis of the First New Batch of IL **7b***

Reference		Sample composition	Temp ℃	Solvent	Analysis	Result
JDH45(1)		**7b**	25	CDCl₃	NMR	
JDH45(2)	[1]	**7b**	25	DMSO	NMR	Positive for CHCl₃
JDH45(2)	[2]	**7b**, TMS	25	DMSO	NMR	

*Spectrum 10: NMR Spectra of the First New Batch of IL **7b***
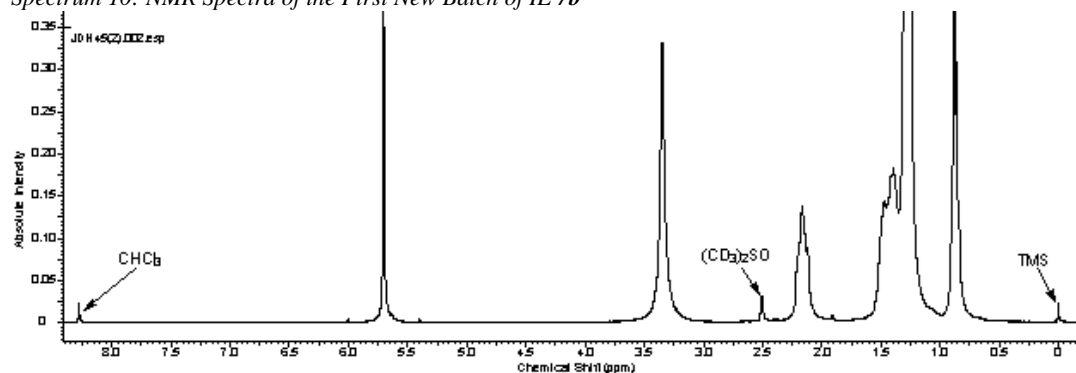
When it was confirmed that there was residual $CHCl_3$, in the new batch of IL **7b**, from separation, we decided to heat it under vacuum. Initially we began heating the IL with a heating mantle under vacuum in a sand bath. However, the temperature was difficult to maintain although we were using a ground glass thermometer that could monitor the temperature inside the flask under vacuum, therefore, we eventually decided to use an oil bath, and found the proper temperature to keep the oil bath that would allow for the IL to reach 85℃ and stay at that temperature. This IL was heated under vacuum for the next 10 hours, and in the meantime, we decided to run other reactions in IL **7b** and use the remaining IL. At this point, we were concerned that many of the rates of each reaction were not comparable because catalyst initiation may be delayed in some, leading to 0% completion within the first few hours. We had some qualitative evidence and quantitative. Qualitatively there would not be any anisole in NMR analysis while the reactions remained a bright amber color, but when the reaction color changed to a dark brown (Figure 9), and formed small bubbles (likely CO_2) there was immediate visualization of anisole in NMR or GC, which had been known since Charbonneau's work.

Figure 9: Qualitative Indication of Reaction Initiation
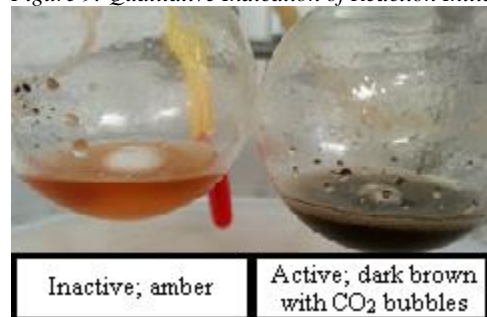
Quantitatively, this catalytic system had been shown to have 1st order kinetics, yet the rates of many reactions were polynomial in the first few hours, then they would level off into a linear rate, this likely suggests that the active catalyst slowly formed over several hours, until it was entirely active. Therefore, we decided to increase the amount of time that we would spin the ligand and $Pd(OAc)_2$ before adding **2** and sodium formate, from 5 minutes to 1 hour and also heat them at 65℃ as described in Experimental 4.

We decided to use the rest of the old IL **7b** at this time. In order to use the old IL we had to move it from a 500 mL round bottom flask to a small 8 mL vial, so the round bottom was suspended and we

allowed gravity to transfer the IL to the vial. However, this was excruciatingly slow, so we decided to heat the outside of the bottle with a heat gun to make it flow quicker after a few hours some of the final IL began bubbling and to have a whit foam over it, and this was discarded. Then **Rxn 24** and **26** were run with ligand **5**, and **Rxn 25** and **27** were run with ligand **4** in IL **7b** that we were able to salvage. With **Rxn 25** there was a logistical problem with placing the condenser, however it ran to 42% when sampled at 21 hours, while **Rxn 24** only ran to 15%. These results were contradictory to most of the samples in IL **7b** thus far, and so we ran an identical set of reactions but they were equally as unreactive over the first five hours with rates of 0.82%/hour and 1.33%/hour as summarized in Table 21 below.

*Table 21: Old IL **7b** after Heating with Heat Gun*

Reaction #	Reference	Reaction Composition	rate (%/hour)
24	JDH 44(1)	**7b:5**	0.50
25	JDH 44(2)	**7b:4**	0.73
26	JDH 47(1)	**7b:5**	0.82
27	JDH 47(2)	**7b:4**	1.33

From these results, we theorized that some contaminant must have entered into the IL that was interfering with the reaction; however, we had tainted and used the remained of that IL, therefore we proceeded to test the new IL **7b** instead. During the process of drying the new IL **7b** molecular sieves accidentally were vacuumed into the IL. The sieves were filtered out, and we proceeded to assess the purity of the IL via NMR while setting up one reaction of that IL with ligand **4** (**Rxn 28**, Table 22) and testing the water content (JDH 48, Table 23). From checking the NMR the IL had a large peak at 1.45-ppm region, and one at 1.89-ppm shown in Spectrum 11 which we could not identify. Additionally, these same peaks were seen in the NMR of the reaction, but they faded over time, as shown in Spectrum 11.

*Spectrum 11: NMR Analysis of Rxn 28 in IL **7b** after Heating under Vacuum with Molecular Sieve Contamination*
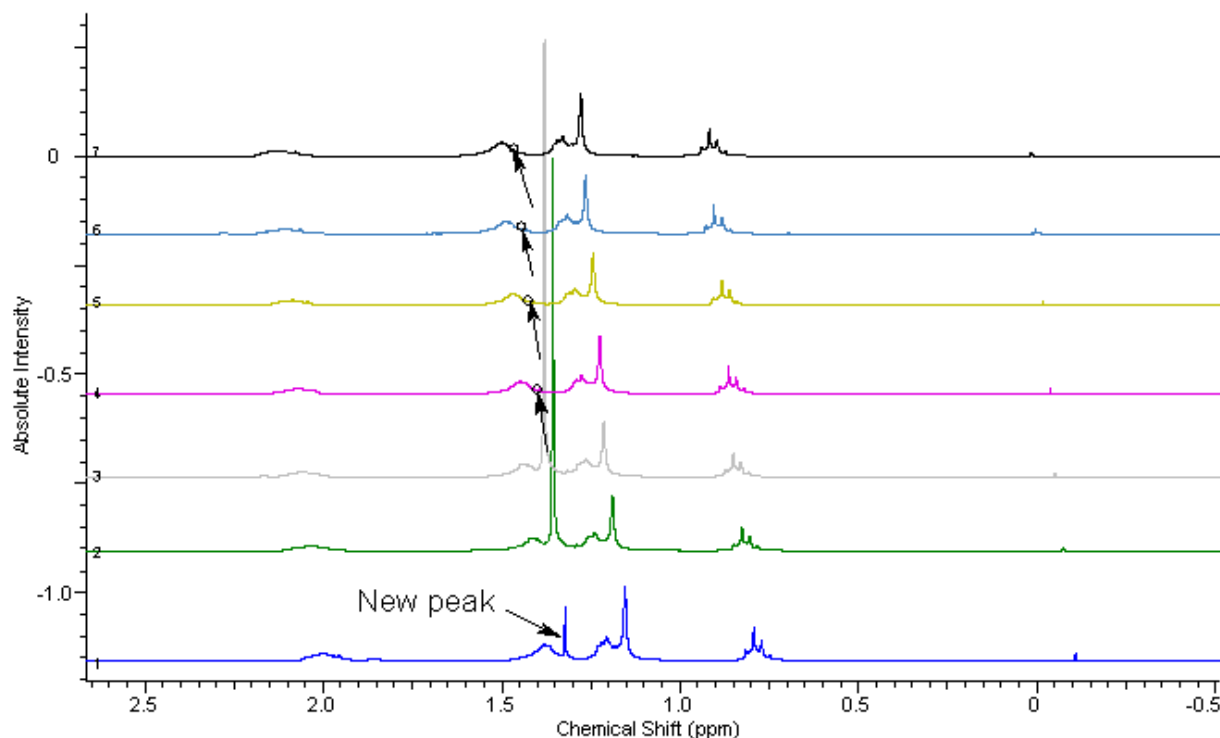
Despite the reaction contaminants, the reaction ran at speeds comparable to previous experiments in IL **7b**

with a rate of 5.3 %/hour only 2%/hour slower than the average reaction in IL **7b** with ligand **4** (Table

22). From the Karl Fischer of this IL as a 10% solution in MeOH there was 0.068 χ_{H_2O}, roughly 23 times

more water than the old IL Table 23.

*Table 22: **Rxn 28** in IL **7b** after Heating under Vacuum with Molecular Sieve Contamination*

Reaction #	Reference	Reaction Composition	rate (%/hour)
28	JDH 48(2)	**7b:4**	5.29

*Table 23: Karl Fischer of IL **7b** after Heating under Vacuum*

Reference	Sample composition	St. Dev. (S)	Mean (S)	% dev S	Avg ppm H₂O	χ_{H_2O}
JDH 48	11.6 % **7b** in CH₃OH	17.3	548.4	3.1%	1717.5	0.068

*This is the second batch of IL **7b**, that was contaminated with molecular sieve after heating under vacuum.*

These Karl Fischer results prompted us to improve how we dried the IL, at this point we placed a stir bar

in the round bottom, to accelerate the heating. Once the stir bar was added, and the IL was being heated,

the IL began to bubble vigorously—whereas without the stir bar, it would bubble minimally—it was

theorized that this bubbling was likely indicative of H₂O boiling off, or other contaminants. At this point

we were using a round bottom flask, with an adapter and vacuum hose with a septum in the top as in Figure 10 Panel A.

Figure 10: Initial Drying Apparatus
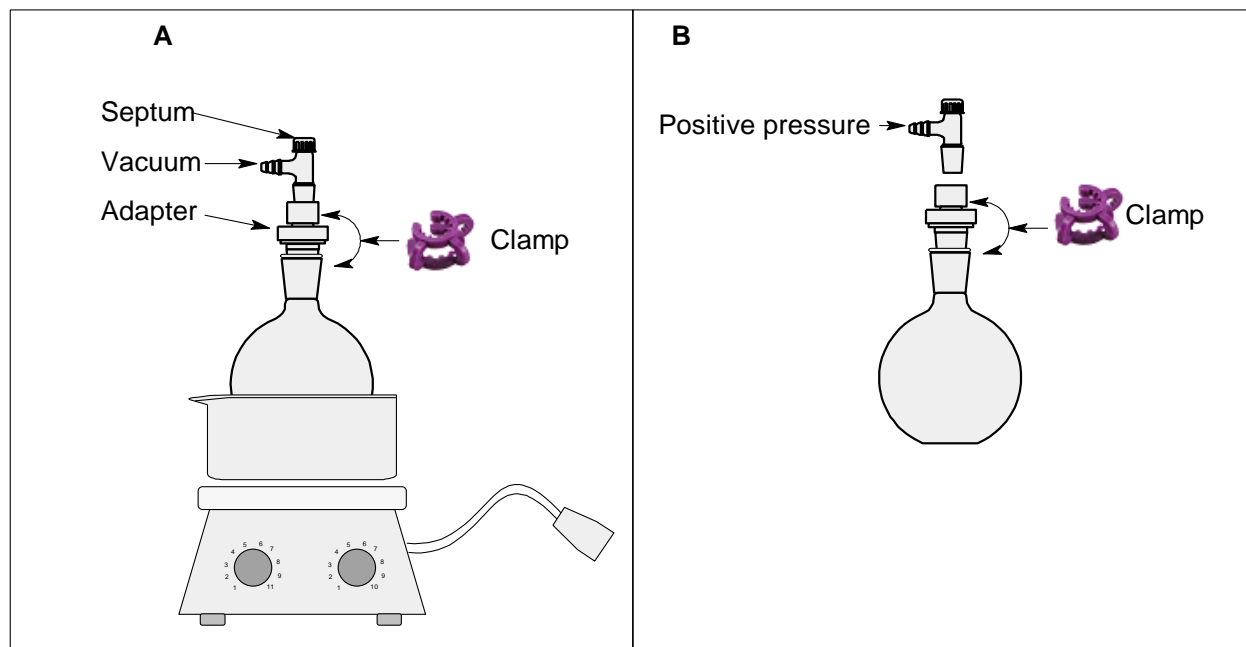
To improve the drying method/extraction of IL for experiments, we wanted to add argon to the chamber while still under vacuum and then be able to take a sample of IL from the top, while it was still warm, using a gas tight syringe to avoid extracting the IL in a cumbersome glove bag. However, the added pressure caused the apparatus to come apart as shown in Figure 10 Panel B. After this we made another sample of IL **7b** and the water was tested after separation showing 11000-ppm so the IL was heated under vacuum overnight in a new apparatus that we developed shown in Figure 11. This apparatus allowed us to finish heating under vacuum then disconnect with minimal risk of atmospheric re-pressurization. In fact, argon could be directly connected and slowly let into the round bottom flask. Then the IL could be drawn from the other opening while flushing with argon, essentially removing any potential for atmospheric H_2O to confound the KF analysis or for oxygen to seep into the IL before adding it to the reactions.

Figure 11: Final IL Drying setup and KF testing

We then tested the IL **7a** that was not heated under vacuum as a neat KF test—as explained in

Experimental 3. This test represented the water content of reactions **9**, **10**, **14**, **17**, and **18**, as none of those

reactions had IL that had been heated under vacuum, and also shed light on how accurate our NMR

analysis of water content was. From this neat analysis of the IL it is apparent that the IL indeed was much

less hygroscopic at only 0.088 χ_{H_2O} (Table 24) compared to the NMR estimate of 0.44 or the average

initial KF estimate of 0.22 ($\approx$2.5 to 5 times less than original estimates from NMR or KF). Nevertheless,

IL **7a** was still clearly more hygroscopic than **7b**, especially given that initial KF titrations likely

overestimated the water concentration of **7b**. From this point forward, we tested the water concentration

before running each experiment, and we heated the IL under vacuum; however, there was still one more

possible factor to control for, and that was the possibility of adding water with the addition of sodium

formate.

Table 24: Initial Karl Fischer Titrations of Neat IL

Reference	Sample composition	St. Dev. (S)	Mean (S)	% dev S	χ_{H_2O}
JDH 51(1)	Old IL **7a**	227.9	3359.6	6.78%	0.088
JDH 51(2)	IL **7b** drying for 12 hours	53.6	60.9	87.98%	0.003
JDH 51(3)	IL **7a** drying 4 hours	140.9	486.9	28.93%	0.014

9. Water Content of $NaCO_2H$

The water content of sodium formate was determined by heating it in a crucible. The complication with

this analysis is that $NaCO_2H$ forms Na_2CO_3 at temperatures exceeding 480 °C,[50] while releasing CO and

H_2. Therefore stoichiometric calculations needed to be considered following the weighing of materials

before and after heating. Scheme 12 below shows the stoichiometric equivalences.

Scheme 12: Decomposition of Sodium Formate at Temperatures Exceeding 480 ℃

$$2\ NaCO_2H \xrightarrow{> 480\ ^oC} Na_2CO_3\ +\ CO\ +\ H_2$$
$$H_2O$$
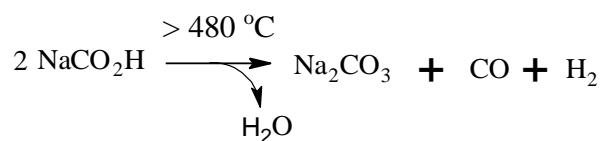
We ran two trials with 272 mg of sodium formate alone, and then one trial with 18.5 uL of H_2O added.

From the first two trials, the average χ_{H_2O} in the sodium formate was 0.0219 (0.6% standard deviation).

From the trial with 18.5 µL of H_2O added it seemed as the water certainly boiled off, but the mass of the

added water was incorrect as this trial suggested that the initial sodium formate had a χ_{H_2O} of -0.0290.

Overall, from this experiment, there was roughly a maximum χ_{H_2O} of 0.0252 in **7a** or 0.305 in **7b**, added

to any reaction.

10. Summary of Results

Below are two graphs, one that shows every hydrodechlorination reaction (Figure 12), and one that excludes compromised reactions (Figure 13). All of the justifications for excluding the results of certain reactions are also tabulated (Table 25). The trends from each set of data are summarized in Figure 14. By excluding obviously compromised reactions, it appears that reactions in IL **7b** proceed faster on average than those in IL **7a** with a 3% confidence, given their standard deviations. However, the sample size of reactions performed in IL **7a** was too small to make reliable comparisons and more trials would need to be performed to confirm this result. Overall, the data suggest that reactions performed with ligand **5** run faster than those with ligand **4**, which confirms work from previous students in Dr. Logan's lab, however the standard deviation between the reactions leave uncertainty in this conclusion.[18]

Additionally, from analyzing the water content of each reaction by using an average reaction rate at each concentration, it appears that there may be a bell curve to the concentration of water vs rate of reaction (Figure 15). However, these results are not all consistent, and suggest a possible future study of the impact of water concentration on reaction rate.

Figure 12: Reaction Rates of Every Reaction That Was Performed
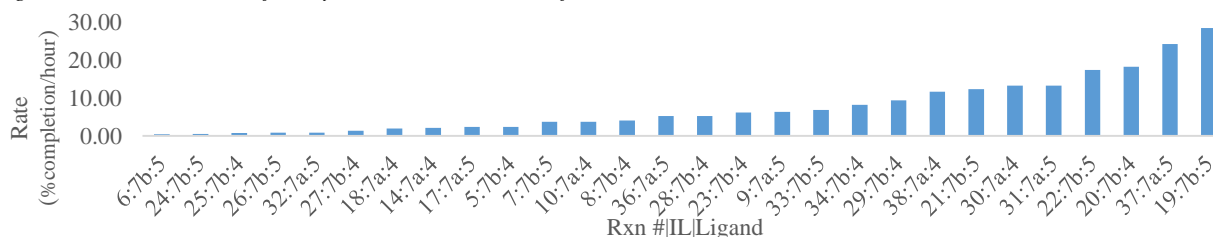
The bottom axis contains the information of the reaction rate represented by that column by stating the Rxn number, character of the IL, and finally the ligand. In this figure each reaction is compared using the rate in %completion /hour, the rates were standardized by excluding samples well beyond the time period appropriate for sampling.

Figure 13: Reaction Rates Excluding Confounded Reactions
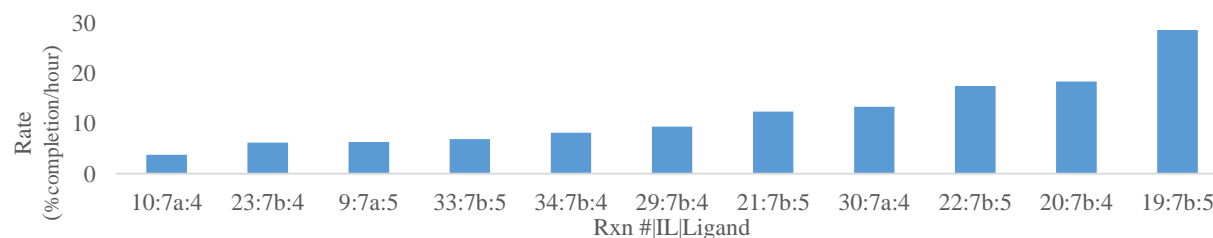
In this figure each reaction is compared using the rate in %completion /hour, the rates were standardized by excluding samples well beyond the time period appropriate for sampling.

Figure 14: Trends from Every Reaction vs Select Reactions
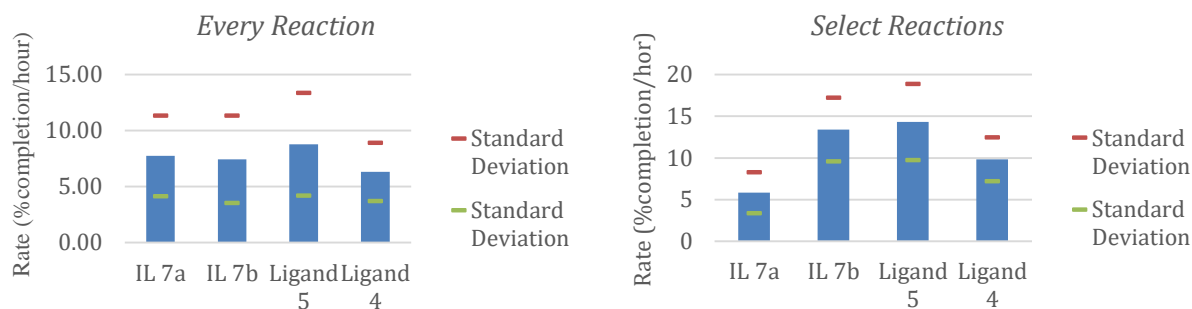
Table 25: Experiments with Confounding Experimental Conditions

Reaction :IL:Ligand	Confounding factor
5:7b:4	Only two time samples
6:7b:5	Only two time samples
7:7b:5	Different reaction temp
8:7b:4	Different reaction temp
14-16:7a:4	Mini NMR/GC Sample
17:7a:5	Poor reaction initiation
18:7a:4	Died early
24:7b:5	IL heated with gun
25:7b:4	IL heated with gun
26:7b:5	IL heated with gun
27:7b:4	IL heated with gun
28:7b:4	Molecular sieves
31:7a:5	Water did not mix in
32:7a:5	Poor reaction initiation
36:7a:5	Double sized reaction
37:7a:5	mol concentration
38:7a:4	mol concentration

Figure 15: Average mole fraction of H_2O vs Rate (%conversion/hour)
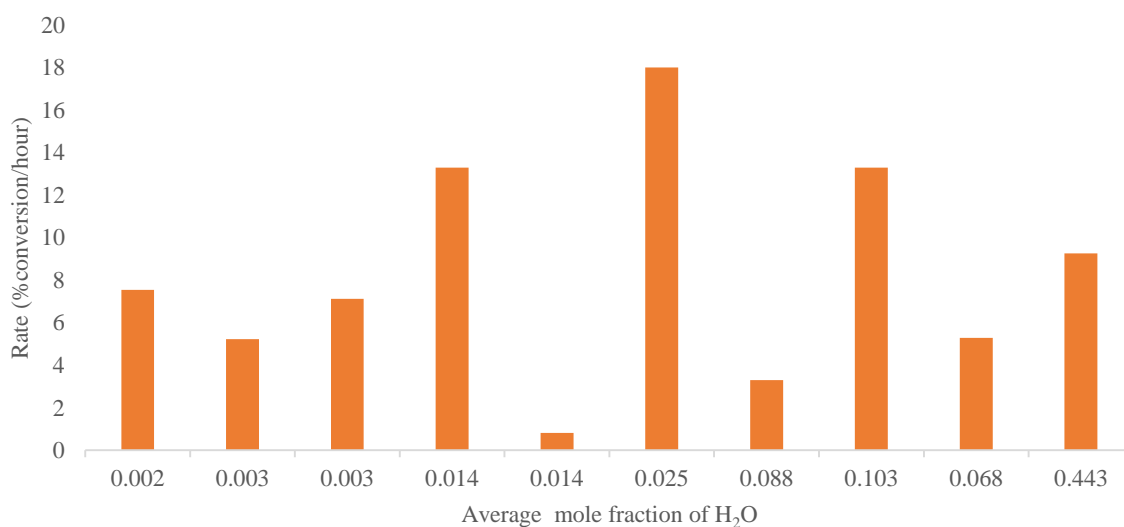
Conclusion

The experimental plan was to test the hydrodechlorination efficacy and longevity of palladium active catalyst with ligands **4** and **5** in ILs **6**, **7a**, and **7b**. Through these experiments, we hoped to determine how the ligand impacts the reaction in ILs, how the anion of the IL impacts the rate of reaction, how the ILs affect the longevity of the catalyst with either ligand, and how these results compare to conclusions drawn by previous students in both methanol and ILs.

However, through the process of this research, we found the following to be true: the presence or absence of water, evaporation of reactants and products, the possibility of side reactions like β-elimination of the alkyl chains on the phosphonium, or other side reactions, had an effect on the results obtained, and their analysis. We were able to control the concentration of water by heating the ILs under vacuum. This required several logistical innovations, such as developing a method to determine the concentration of water in neat IL by Karl Fischer titration, instead of using a 10% solution in methanol; and arranging the reaction apparatus to keep the IL from interacting with the atmosphere as much as possible. We were able to improve the reaction conditions and sampling technique to reduce the amount of product/reactant that would evaporate between sampling by carefully monitoring the argon flow, and by swapping septa between sampling and while sampling, thus never leaving the reaction uncovered. Of note, we would presume that the anisole evaporates more quickly based on boiling point, which correlates with vapor pressure, yet we could not prove whether the anisole or 4-chloroanisole was evaporating faster. We were able to find an appropriate temperature (80°C) to run the reactions and follow by NMR in a convenient timeframe. Development of the NMR analysis provided a way to efficiently analyze hydrodechlorination reactions in phosphonium ILs using NMR spectrometry. We ruled out the use of GC for analyzing hydrodechlorination reactions based on efficiency of GC sample preparation vs NMR sample preparation. All of the aforementioned experiments also revealed that the reactants and products of the reaction might be evaporating over time, which was confirmed by testing the suspected sample evaporation. This is another area of possible future research.

Unfortunately, we could not find a set of conditions that reliably caused the reaction to initiate at a consistent rate, but we attempted to control it by increasing the time spent stirring the ligand and palladium before adding the other reagents, which was minimally effective. However, with the improved logistics of drying the ILs and analyzing their water content by Karl Fischer titration; reducing reactant and product evaporation by using a septum during reaction sampling; and an improved NMR method for analyzing reaction progress, research to confirm some of the tentative conclusions reached during this thesis research will be enabled.

References

(1)   Meharg, A. A.; Killham, K. *Nature* **2003**, *421* (6926), 909.

(2)   US EPA, O. Learn about Polychlorinated Biphenyls (PCBs) https://www.epa.gov/pcbs/learn-about-polychlorinated-biphenyls-pcbs (accessed Jun 9, 2016).

(3)   Porta, M.; Zumeta, E. *Occup. Environ. Med.* **2002**, *59* (10), 651–652.

(4)   Faroon, O.; World Health Organization; United Nations Environment Programme; International Labour Organisation; Inter-Organization Programme for the Sound Management of Chemicals; International Program on Chemical Safety. *Polychlorinated biphenyls: human health aspects*; World Health Organization: Geneva, 2003.

(5)   Van den Berg, M.; Birnbaum, L.; Brunström, B.; Cook, P.; Feeley, M.; Giesy, J. P.; Hanberg, A.; Hasegawa, R.; Kennedy, S. W.; Kubiak, T.; Larsen, J. C.; Nolt, C.; Peterson, R. E.; Poellinger, L.; Safe, S.; Schrenk, D.; Tillitt, D.; Tysklind, M.; Younes, M.; Wærn, F.; Zacharewski, T. *Environ. Health Perspect.* **1998**, *106* (12), 775–792.

(6)   Chernyak, Y. I.; Shelepchikov, A. A.; Brodsky, E. S.; Grassman, J. A. *Toxicol. Lett.* **2012**, *213* (1), 9–14.

(7)   Aliyu, M. H.; Alio, A. P.; Salihu, H. M. *J. Environ. Health* **2010**, *73* (3), 8.

(8)   Ikeda, M. *Chemosphere* **1996**, *32* (3), 559–566.

(9)   Masuda, Y. *Chemosphere* **2001**, *43* (4–7), 925–930.

(10)   Drexler, H.; Kerscher, G.; Angerer, J. *Gesundheitswesen* **2004**, *66*, 47–51.

(11)   Tarr, M. A. *Chemical Degradation Methods for Wastes and Pollutants: Environmental and Industrial Applications*; CRC Press, 2003.

(12)   *Environ. Sci. Technol.* **2002**, *36* (11), 231A–235A.

(13)   EPA, U. Hudson River Cleanup | Hudson River PCBs Superfund Site | US EPA https://www3.epa.gov/hudson/cleanup.html#quest1 (accessed May 26, 2016).

(14)   Connors, T. F.; Rusling, J. F. *Chemosphere* **1984**, *13* (3), 415.

(15)   Chang, B. V.; Chou, S. W.; Yuan, S. Y. *Chemosphere* **1999**, *39* (1), 45–54.

(16)   Bunge, M.; Adrian, L.; Kraus, A.; Opel, M.; Lorenz, W. G.; Andreesen, J. R.; Görisch, H.; Lechner, U. *Nature* **2003**, *421* (6921), 357–360.

(17)   Fava, F.; Marchetti, L. *Appl. Microbiol. Biotechnol.* **1991**, *36* (2), 240.

(18)   Logan, M. E.; Oinen, M. E. *Organometallics* **2006**, *25* (4), 1052–1054.

(19)   Chen, J.; Zhang, Y.; Yang, L.; Zhang, X.; Liu, J.; Li, L.; Zhang, H. *Tetrahedron* **2007**, *63* (20), 4266–4270.

(20)   Milstein, D.; Ben-David, Y.; Gozin, M.; Portnoy, M. *J. Mol. Catal.* **1992**, *73* (2), 173–180.

(21)   Collman, J. P.; Hegedus, L. S.; Norton, J.; Finke, F. *Principles and applications of organotransition metal chemistry*; University Science Books: Mill Valley, Calif, 1987.

(22)   Portnoy, M.; Milstein, D. *Organometallics* **1993**, *12* (5), 1665–1673.

(23)   Portnoy, M.; Milstein, D. *Organometallics* **1993**, *12* (5), 1655–1664.

(24)   Otsuka, S. *J. Organomet. Chem.* **1980**, *200* (1), 191–205.

(25)   Hartwig, J. F. *Angew. Chem. Int. Ed.* **1998**, *37* (15), 2046–2067.

(26)   Buchwald, S. L.; Wolfe, J. P. *Angew. Chem. Int. Ed.* **1999**, *38* (16), 2413–2416.

(27)   Buchwald, S. L.; Barder, T. E.; Walker, S. D.; Martinelli, J. R. *J. Am. Chem. Soc.* **2005**, *127* (13), 4685–4696.

(28)   Hartwig, J. F.; Paul, F. *J. Am. Chem. Soc.* **1995**, *117* (19), 5373–5374.

(29)   Parrish, C. A.; Buchwald, S. L. *J. Org. Chem.* **2001**, *66* (11), 3820–3827.

(30)   de Vries, J. G. *Dalton Trans* **2006**, No. 3, 421–429.

(31)   Reetz, M. T.; de Vries, J. G. *Chem. Commun.* **2004**, No. 14, 1559.

(32)   Dupont, J.; Cassol, C. C.; Umpierre, A. P.; Machado, G.; Wolke, S. I. *J. Am. Chem. Soc.* **2005**, *127* (10), 3298–3299.

(33)   Finke, R. G.; Widegren, J. A. *J. Mol. Catal. Chem.* **2003**, *198* (1–2), 317–341.

(34)   Phan, N. T. S.; Van Der Sluys, M.; Jones, C. W. *Adv. Synth. Catal.* **2006**, *348* (6), 609–679.

(35)   *Organometallic chemistry*; Fairlamb, I., Lynam, J., Royal Society of Chemistry (Great Britain), Eds.; Specialist periodical report; The Royal Society of Chemistry: Cambridge, UK, 2016.
(36)   Kurokhtina, A. A.; Schmidt, A. F. *Arkivoc* **2009**, *2009* (11), 185.
(37)   Glasnov, T. N.; Findenig, S.; Kappe, C. O. *Chem. - Eur. J.* **2009**, *15* (4), 1001–1010.
(38)   Kaufmann, D. E.; Nouroozian, M.; Henze, H. *Synlett* **1996**, *1996* (11), 1091–1092.
(39)   Foley, P.; DiCosimo, R.; Whitesides, G. M. *J. Am. Chem. Soc.* **1980**, *102* (22), 6713–6725.
(40)   Crabtree, R. H.; Anton, D. R. *Organometallics* **1983**, *2* (7), 855–859.
(41)   Xu, S.; Yang, Q. *J. Phys. Chem. C* **2008**, *112* (35), 13419–13425.
(42)   Zhang, C.; Li, X.; Sun, H. *Inorganica Chim. Acta* **2011**, *365* (1), 133–136.
(43)   Buchwald, S. L.; Wolfe, J. P.; Tomori, H.; Sadighi, J. P.; Yin, J. *J. Org. Chem.* **2000**, *65* (4), 1158–1174.
(44)   Strieter, E. R.; Blackmond, D. G.; Buchwald, S. L. *J. Am. Chem. Soc.* **2003**, *125* (46), 13978–13980.
(45)   Martin H. G. Prechtl, J. D. S. **2011**.
(46)   Dupont, J.; Scholten, J. D. *Chem. Soc. Rev.* **2010**, *39* (5), 1780–1804.
(47)   Del Sesto, R. E.; Corley, C.; Robertson, A.; Wilkes, J. S. *J. Organomet. Chem.* **2005**, *690* (10), 2536–2542.
(48)   Ghandi, K.; Dwan, J.; Durant, D. *Open Chem.* **2008**, *6* (3).
(49)   Gottlieb, H. E.; Kotlyar, V.; Nudelman, A. *J. Org. Chem.* **1997**, *62* (21), 7512–7515.
(50)   Boswell, M. C.; Dickson, J. V. *J. Am. Chem. Soc.* **1918**, *40* (12), 1779–1786.

Acknowledgements

I would first like to thank my thesis advisor Dr. Margret E. Logan, PhD, Associate Professor and Chair of the Department of Chemistry and Biochemistry at the State University of New York The College at Brockport. Dr. Logan's office was always open whenever I ran into a trouble or had a question about my research or writing. She consistently allowed this paper to be my own work, but steered me in the right the direction whenever she thought I needed it.

I would also like to acknowledge the Ronald E. McNair Post-Baccalaureate Achievement Program for providing funding for this research, and Shawn Dirx for completing the initial experiments with me. I am gratefully indebted to their contributions to this thesis.

Finally, I must express my very profound gratitude to my parents and to my many friends for providing me with unfailing support and continuous encouragement throughout my years of study and through the process of researching and writing this thesis. This accomplishment would not have been possible without them. Thank you.

Joseph Hennig

Addendum
Method Information

Method: C:\CHEM32\1\METHODS\MEL_ANISOLE.M Modified: 6/5/2014 at 4:28:31 PM

Method Audit Trail

Operator   : Mlogan

Date   : 2/12/2014 5:26:43 PM

Change Info: This method was created at 2/12/2014 5:26:43 PM and based on

method C:\CHEM32\1\METHODS\MEL_ANISOLE.M

Operator   : Mlogan

Date   : 2/12/2014 5:26:45 PM

Change Info: Method saved. User comment: ""

Operator   : Mlogan

Date   : 2/26/2014 5:01:51 PM

Change Info: Method saved. User comment: ""

Operator   : Mlogan

Date   : 3/5/2014 2:10:16 PM

Change Info: Method saved. User comment: ""

Operator   : JDH

Date   : 6/5/2014 3:36:55 PM

Change Info: Method saved. User comment: ""

Operator   : JDH

Date   : 6/5/2014 4:18:38 PM

Change Info: Method saved. User comment: ""

Operator   : JDH

Date   : 6/5/2014 4:28:31 PM

Change Info: Method saved. User comment: ""

Run Time Checklist

Pre-Run Cmd/Macro: off

Data Acquisition: on

Standard Data Analysis: on

Customized Data Analysis: off

Save GLP Data: off

Post-Run Cmd/Macro: off

Save Method with Data: off

Injection Source and Location

Injection Source: GC Injector

Injection Location: Front

==

==

6890 GC METHOD

==

==

OVEN

0

1 20.00   210   0.00

2   0.0(Off)

Post temp: 50 'C

Post time: 0.00 min

Run time: 8.00 min

FRONT INLET (SPLIT/SPLITLESS)   BACK INLET (UNKNOWN) Mode: Split

Initial temp: 250 'C (On) Gas type: Helium

COLUMN 1   COLUMN 2

Capillary Column   (not installed)

Model Number: Agilent 19091J-413

HP-5 5% Phenyl Methyl Siloxane

Max temperature: 325 'C

Nominal length: 30.0 m

Nominal diameter: 320.00 um

Nominal film thickness: 0.25 um

Inlet: Front Inlet

Outlet: Front Detector

FRONT DETECTOR (FID)   BACK DETECTOR (NO DET) Temperature: 250 'C (On)

Hydrogen flow: On Air flow: On Makeup flow: On

Makeup Gas Type: Helium

Flame: On

Electrometer: On

Lit offset: 2.0

SIGNAL 1   SIGNAL 2

Data rate: 20 Hz   Data rate: 20 Hz

Type: front detector   Type: front detector

Save Data: On   Save Data: Off

Zero: 0.0 (Off)   Zero: 0.0 (Off)

Range: 0   Range: 0

Fast Peaks: Off   Fast Peaks: Off

Attenuation: 0   Attenuation: 0

COLUMN COMP 1   COLUMN COMP 2

Derive from front detector   Derive from front detector

POST RUN

Post Time: 0.00 min

TIME TABLE

Time   Specifier   Parameter & Setpoint

GC Injector

Front Injector:

Sample Washes   2

Sample Pumps   6

Injection Volume   1.00 microliters Syringe Size   10.0 microliters Nanoliter Adapter

On

PreInj Solvent A Washes   0

PreInj Solvent B Washes   0

PostInj Solvent A Washes   2

PostInj Solvent B Washes   0

Viscosity Delay   0 seconds

Plunger Speed   Fast

PreInjection Dwell   0.00 minutes

PostInjection Dwell   0.00 minutes

Back Injector:

No parameters specified

== The

Acq. Method's Instrument Parameters for the Run were :

no Run specific Instrument Parameter Listing exists

The Data Analysis Parameters of the used Method are :

===

Integration Events

===

-- Non signal specific Integration Events

Event	Value
Tangent Skim Mode	Standard
Tail Peak Skim Height Ratio	0.000
Front Peak Skim Height Ratio	0.000
Skim Valley Ratio	20.000
Baseline Correction	Classical
Peak to Valley Ratio	500.000

-- Default Integration Event Table "Event"

Event	Value	Time
Initial Slope Sensitivity	1.000	Initial
Initial Peak Width	0.040	Initial
Initial Area Reject	1.000	Initial
Initial		
Initial Height Reject		
Shoulders	1.700	
OFF Initial		
Initial		

-- Detector Default Integration Event Table

"Event_TCD"

Event   Value   Time

|--|------------|-------|

Initial   Slope Sensitivity   100.000Initial

Initial   Peak Width   0.040   Initial

Initial   Area Reject   1.000   Initial

Initial

Initial   Height Reject

Shoulders   1.000

OFF   Initial

Initial

-- Detector Default Integration Event Table

"Event_ADC"

Event   Value   Time

|--|------------|-------|

Initial   Slope Sensitivity   20.000 Initial

Initial   Peak Width   0.040   Initial

Initial   Area Reject   1.000   Initial

Initial

Initial   Height Reject

Shoulders   1.000

OFF   Initial

Initial

-- Detector Default Integration Event Table

"Event_ECD"

Event   Value   Time

|---|------------|-------|

-- Detector Default Integration Event Table

"Event_NPD"

Event   Value   Time

|---|------------|-------|

Initial   Slope Sensitivity   500.000Initial

Initial   Peak Width   0.040   Initial

Initial   Area Reject   1.000   Initial

Initial

Initial   Height Reject

Shoulders   1.000

OFF   Initial

Initial

-- Detector Default Integration Event Table

"Event_FPD"

Event		Value	Time
Initial	Slope Sensitivity	50.000	Initial
Initial	Peak Width	0.040	Initial
Initial	Area Reject	1.000	Initial
Initial			
Initial	Height Reject		
Shoulders	1.000		
OFF	Initial		
Initial			

-- Detector Default Integration Event Table

"Event_uECD"

Event	Value	Time
Initial Slope Sensitivity	500.000	Initial
Initial Peak Width	0.080	Initial
Initial Area Reject	1.000	Initial
Initial Height Reject	1.000	Initial

Initial Shoulders

Baseline Now   OFF   Initial

3.700

Integration   ON   3.700

Baseline Hold   ON   3.900

Integration   ON   5.300

Baseline Hold   ON   5.500

--- Detector Default Integration Event Table

"Event_FID"

Event	Value	Time
Integration	OFF	5.500

Apply Method's Manual Integration Events: No

=== Specify

Report

===

Calculate: Area Percent

Use Multiplier & Dilution Factor with ISTDs

Use Sample Data from Data File

Destination: Printer, Screen

Quantitative Results sorted by: Signal

Report Style: Short

Sample info on each page: No

Add Chromatogram Output: Yes

Chromatogram Output: Portrait

Size in Time direction: 100 % of Page

Size in Response direction: 25 % of Page

Uncalibrated Peaks: Report with Calibrated Peaks

=== Signal

Options

===

Include: Axes, Retention Times, Baselines, Tick Marks

Font: Arial, Size: 8

Ranges: Full

Multi Chromatograms: Separated, Each in full Scale

==

Calibration Table

==

Calib. Data Modified :

Rel. Reference Window :   5.000 % Abs. Reference Window :   0.000 min Rel. Non-ref. Window :

5.000 % Abs. Non-ref. Window :   0.000 min

Uncalibrated Peaks   :   not reported

Partial Calibration   :   Yes, identified peaks are recalibrated

Correct All Ret. Times: No, only for identified peaks

Curve Type   :   Linear Origin   :   Included Weight   :   Equal

Recalibration Settings:

Average Response   :   Average all calibrations

Average Retention Time: Floating Average New 75%

Calibration Report Options :

Printout of recalibrations within a sequence:

Calibration Table after Recalibration

Normal Report after Recalibration

If the sequence is done with bracketing:

Results of first cycle (ending previous bracket)

Signal 1: NEW, anisole

Signal 2: NEW, chloroanisole

=== Peak

Sum Table

===

No Entries in table

===

==

Sample related custom fields

==

Custom Field   Type   Mand. Default Value

None defined

==

Compound related custom fields

==

Custom Field   Type   Mand. Default Value

None defined